FACULTY OF INFORMATION TECHNOLOGY AND ELECTRICAL ENGINEERING

DEGREE PROGRAMME IN RADIO ENGINEERING

MASTER'S THESIS

Development of Interconnections for mm-Wave Antenna Module Package

Author	Olli Manninen
Supervisor	Markus Berg
Second Examiner	Sami Myllymäki
Technical Advisor	Tero Kangasvieri

May 2019

Manninen O. (2019) Development of Interconnections for mm-Wave Antenna Module Package. University of Oulu, Degree Programme in Radio Engineering. Master's Thesis, 66 p.

ABSTRACT

The increase in mobile network data usage has led to interests in mm-wave frequencies (for example 26.5 GHz – 29.5 GHz) on becoming fifth generation (5G) networks in addition to previously used sub-6 GHz frequencies. The advantage of mm-wave frequencies is larger bandwidth, leading to larger throughput with a tradeoff of smaller coverage due to shorter wavelength. The coverage issue can be compensated by using antenna arrays instead of one antenna. There have been some studies about stacking antenna module package vertically on motherboard, and in more advanced approach, the RFIC is integrated into the bottom of the antenna module package.

This thesis concentrates on developing the interconnection between two PWBs on mm-wave frequency (26.5 GHz – 29.5 GHz) between the antenna module and motherboard. More accurately, creating interconnection around via structure, carrying RF-signal from antenna module to motherboard by applying vertical stacking. This method may reduce the overall price of the system, while increasing the level of integration in the system. The overall aim of this thesis was to provide a functional and optimized interconnection method with measurement results and limitations of Nokia Factory.

The interconnection can be created by using electromagnetic coupling or galvanic connection. The galvanic connection was chosen for many reasons and different interconnection methods applying galvanic connection were introduced. These methods include LGA and BGA soldering, traditional RF-connector and antenna array connector with 16-ports. After considering the options and Nokia Factory limitations, the most suitable interconnection method turned out to be LGA soldering.

The research work includes partial design of antenna module and motherboard, and the optimization for connection. Prototypes were created based on the design, and the measurement results and conclusions of interconnection functionality were provided as well. Six prototypes were made, from which prototypes 3-6 were functional in terms of solder height. The measurement results show that there was variation in matching between different prototypes and between simulation and measurement results. By doing x-ray and failure analysis, a few reasons were found to explain the variation. One reason can be found from voids in signal soldering, which widens the soldering horizontally, leading to decreased matching due to changed solder diameter and asymmetric grounding. However, by utilizing the solder bumping method, the appearance and diameter of voids can be minimized.

The conclusion with prototypes was that the system functions well, but improvements are recommended, and simulations should be re-done with modifications from failure analysis. Overall, the aim of the thesis was reached.

Keywords: antenna array, array connector, interconnection, mm-wave, vertical stacking

Manninen O. (2019) Antennimoduulipaketin Liitäntöjen Kehittäminen Millimetriaalto Taajuuksille. Oulun Yliopisto, Tieto- ja Sähkötekniikan Tiedekunta, Radiotekniikan opinto-ohjelma, Diplomityö, 66 s.

TIIVISTELMÄ

Datankäytön jatkuvan kasvun takia viidennen sukupolven (5G) matkapuhelinteknologian kehitys on keskittynyt aiemmin käytettyjen alle 6 GHz taajuuksien lisäksi uusille, korkeammille, millimetriaaltojen (esim. 26.5 GHz – 29.5 GHz) taajuuskaistalle. Korkeammat taajuudet tarjoavat mahdollisuuden käyttää suurempia kaistanleveyksiä kasvattaen läpikulkevan datan määrää, mutta sen hintana on signaalin kantomatkan pienentyminen aallonpituuden pienentymisen takia. Kantomatkan lyhenemistä voidaan kuitenkin kompensoida käyttämällä antenniryhmiä yksittäisten antennien asemasta. Antenniryhmien integroinnista systeemiin on tehty erilaisia tutkimuksia, joita ovat esimerkiksi vertikaalinen pinoaminen, jossa antennilevy juotetaan toiselle piirilevylle. Edistyksellisemmässä versiossa kyseisen antennilevyn pohjaan on liitetty RFIC piiri.

Tässä diplomityössä tutkittiin kahden piirilevyn välistä liityntäkohtaa vertikaalisella pinoamisella. Liityntäkohta kuljettaa millimetriaaltotaajuista RF-signaalia (26.5 GHz – 29.5 GHz) antennilevyltä äitilevylle. Kyseisellä rakenteella voidaan saada pienennettyä mahdollisen tuotteen kustannuksia, samalla pienentäen myös sen fyysistä kokoa. Työn tarkoituksena on tarjota Nokialle valmiiksi optimoitu liitäntäratkaisu mittaustuloksineen ja tuotannon rajoitteineen dokumentoituna.

Tutkittu liityntäkohta voidaan muodostaa sähkömagneettisella kytkeytymisellä tai galvaanisesti, joista jälkimmäinen on huomattavasti järkevämpi ja tässä työssä on esitetty sille erilaisia vaihtoehtoja , joita on vertailtu toisiinsa. Näihin vaihtoehtoihin sisältyy koneellinen juottaminen LGA tai BGA tavalla, RF-liittimien käyttö ja antenniryhmää varten kehitetty 16 porttinen liitin. Kyseisistä liitäntä vaihtoehdoista parhaaksi ja soveltuvimmaksi osoittautui LGA juotos.

Tutkimustyö sisältää antennilevyn ja äitilevyn osittaisen suunnittelun ja optimoinnin, ja sen perusteella tehdyn prototyypin, mittaustulokset ja päätelmät liitynnän toimivuudesta. Prototyyppejä tehtiin kaikkiaan kuusi, joista viimeiset 3-6 olivat onnistuneita juotospaksuuden perusteella. Mittausten perusteella sovituksessa on paljon vaihtelua, jolle löydettiin muutamia syitä röntgen tarkastuksessa ja virheanalyysissa. Näihin syihin sisältyy juotoksesta löytyneet kaasukuplat, jotka johtavat juotoksen laajenemiseen horisontaalisesti, mikä taas heikentää maadoitusta ja täten sovitusta. Juotoksen kaasukuplat voidaan kuitenkin välttää niin kutsutulla juotoksen pallottamisella (Engl. Solder Bumping), jossa kaasukuplia ilmeni huomattavasti vähemmän ja ne olivat pienempiä.

Lopputulemana todettiin, että työ on onnistunnut ja prototyyppi on toimiva, mutta tarjotut kehitysideat kannattaa huomioida mahdollisessa jatkokehityksessä ja simuloinnit tulisi tehdä uudelleen virheanalyysistä saaduilla arvoilla ja tiedoilla.

Avainsanat: antenniryhmä, array-liitin, millimetriaalto, vertikaalinen pinoaminen

TABLE OF CONTENTS

ABSTRACT
TIIVISTELMÄ
TABLE OF CONTENTS
PREFACFE
LIST OF ABBREVIATIONS AND SYMBOLS
1 INTRODUCTION 8
2 THEORETICAL BACKGROUND 10
2.1 Antenna 10
2.1.1 Microstrip patch antenna 10
2.1.2 Antenna array 11
2.1.3 Radio Frequency Integrated Circuit - RFIC 12
2.1.4 Grounded Coplanar Waveguide - GCPW 12
2.2 Broadband impedance matching 13
2.2.1 Scattering parameters 13
2.2.2 Broadband impedance matching 15
3 INTERCONNECTION OPTIONS BETWEEN ANTENNA MODULE AND MOTHERBOARD 17
3.1 The antenna modules as Surface Mounted Devices 17
3.1.1 Machinery soldering process 17
3.1.2 Land-Grid Array – LGA 19
3.1.3 Ball-Grid Array – BGA 20
3.1.4 Comparison between LGA and BGA 21
3.2 RF-connector 21
3.3 Antenna Array Connector - Molex 22
4 OPTIMIZING THE CONNECTION 24
4.1 Design 24
4.1.1 PWB materials and stack-up 24
4.1.2 GCPW-via-GCPW and GCPW-via-antenna 26
4.1.3 Antenna module 28
4.1.4 Motherboard 30
4.1.5 Soldering between antenna module and motherboard 31
4.2 Optimization using CST 32
4.2.1 GCPW-via-GCPW optimization 33
4.2.2 GCPW-via-antenna optimization 36
4.3 Optimization using modeFRONTIER optimizing software 38
4.4 Test with final layout 40
5 PROTOTYPE, MANUFACTURING AND MEASUREMENTS 43
5.1 Prototype 43
5.2 Measurements and results 47
5.3 Failure analysis 51
6 DISCUSSION 60

7 CONCLUSIONS 61
8 REFERENCES 63
9 ATTACHMENTS 66

PREFACE

This Master's thesis research was done at Nokia Networks and Solutions in Oulu. The research carried out in this thesis belongs to the 5G millimeter-wave radio research and development.

I am truly grateful to people in Nokia for helping me with my research work, especially to a talented engineer with long experience and thorough knowledge about RF-design, namely D.Sc. (Tech) Tero Kangasvieri. Thank you Tero, for teaching me a lot of useful knowledge about RF-designing and for guiding me through the research work. I also want to thank the talented antenna designer M.Sc. (Tech) Antti-Heikki Niemelä, for helping me with modelling and simulations. Special thanks to layout designer B.Eng. Olli-Antti Laine for doing really good work and being flexible with time schedule.

As to supervisors from the University of Oulu, I want to thank both, D.Sc. (Tech) Markus Berg and D.Sc. (Tech) Sami Myllymäki. Thank you for the good guidance to writing, and more importantly, for commenting my work and giving good guidance around the topic.

I also want to thank my family for supporting me during my studies, my fellow students from unforgettable studying years with them, and finally, my girlfriend Jonna for the support during both studies and research work.

Oulu 3.5.2019

Olli Manninen

LIST OF ABBREVIATIONS AND SYMBOLS

5G	Fifth Generation
AiP	Antenna-in-Package
AM	Antenna Module
AoC	Antenna-on-Chip
BGA	Ball Grid Array
CST	Computer Simulation Technology
GCPW	Grounded Coplanar Waveguide
IF	Intermediate Frequency
LGA	Land Grid Array
LO	Local Oscillator
MB	Motherboard
MOGA	Multi-Objective Genetic Algorithm
ODB++	Open Database++ (data exchange format)
PBGA	Plastic Ball Grid Array
PWB	Printed Wiring Board
RF	Radio Frequency
RFIC	Radio Frequency Integrated Circuit
RX	Receiver
SMD	Surface Mount Device
SMT	Surface Mount Technology
TX	Transmitter
Γ	Reflection Coefficient
tan δ	Loss Tangent
ε_r	Dielectric Constant
λ	Wavelength
Ω	Ohm
D	Horizontal Separation between Signal and Ground
dB	Decibel
H	Distance between Patch and Ground Plane
H_S	Soldering Height between Antenna Module and Motherboard
R_S	Series Resistor (input)
R_L	Load Resistor
S_{XY}	S-parameter, x = receiving port, y = transmitting port
T	Thickness of Conducting Layer in GCPW-line
$T_{MB/AM}$	Thickness of Motherboard or Antenna Module
T_P	Thickness of the Whole Prototype
V_{in}	Input Voltage
Z_0	Characteristic Impedance
Z_L	Load Impedance
W	Width of Signal Trace

1 INTRODUCTION

In recent years, the millimeter waves (mm-waves) have been in great interest in the field of wireless communication [1]. The importance of mm-wave frequencies is highlighted in fifth generation (5G) mobile network, where more bandwidth is required due to a rapidly increasing amount of transferred data [2]. The broader frequency bandwidth is achieved by using mm-wave frequencies, making mm-waves a huge advantage in 5G cellular networks [1].

However, one of the challenges of 5G mm-wave radios comes from increased frequency, which in its turn means decreased wavelength. Decreasing wavelength leads to increased losses in signal path and to increased noise floor. To compensate increased losses and noise floor, higher gain and narrower, more directed, beams are required. The higher gain and directivity can be achieved by using the antenna arrays that can be created to comparably small dimensions. Smaller dimensions lead to an increased level of integration in the final product. [1][2]

Going towards 5G mm-wave radios, a high level of integration in radios is achieved by reducing volume, weight and by using dual-polarized antennas [3]. The latest studies of volume and cost reduction concentrate on vertical stacking integration and packaging solutions [4]. The vertical stacking includes integrating a passive antenna matrix in the package, which is later connected to the main board. This integration is called antenna-in-package (AiP) [4]. In more recent studies, the AiP method is expanded by integrating RFIC (Radio Frequency Integrated Circuit) under the passive antenna matrix package leading to so-called antenna-on-chip (AoC) [4]. In this kind of approach, the cooling for RFIC is utilized by adding cut-offs to motherboard PWB, underneath the RFIC, for heat sink installation [5][6].

In this thesis, interconnection methods are discussed and developed for connecting the 16 pcs of mm-wave (26.5 GHz – 29.5 GHz) 4x4 stacked patch antenna module (AM) PWBs (Printed Wiring Board) (21.1 mm x 21.1 mm x 1.356 mm) to the motherboard (MB) PWB (125 mm x 127.1 mm x 2.158 mm). Fig. 1 illustrates the system under development. Using the most suitable interconnection method, antenna modules are connected to the motherboard and the connection is optimized for the best possible performance. After optimization, the prototype of system is manufactured and measured, and the measurement results are compared to simulation results.

The overall aim of this thesis is to provide an optimized interconnection method with simulation results, the limitations of Nokia production, and finally, documentation of prototype and its functionality. Additionally, the usage of non-mm-wave PWB material is investigated for mm-wave frequency usage to increase the cost-efficiency. The interconnection is optimized for given PWB stack-ups. The achieved results from this thesis may lead to decreased product size and an increased level of integration with increased cost-efficiency in a possible 5G products.

Chapter 2 introduces theoretical background that is needed in the design work and Chapter 3 different connection methods between antenna module and motherboard, and the properties of methods are discussed as well. Also, a short introduction to machinery component soldering is included. Chapter 3 is divided into three sub-chapters, including surface mounted devices

(SMD) as a connection method, RF (Radio Frequency) -connectors and Molex antenna array connector.

In Chapter 4, the design part for antenna modules and motherboard are shown and the most suitable interconnection method is utilized. In that chapter, the whole design procedure is introduced, and motherboard PWB-material functionality is tested for mm-wave frequencies. The optimization process for prototype design is done using CST-simulation software (Computer Simulation Technology) and the final optimization is done by using modeFRONTIER-optimization software. Chapter 5 deals with prototype manufacturing, RF-measurements, comparison of measurement results to simulated ones and analysis of functionality of prototype. The possible reasons for differences between simulation and measurements are searched for by doing failure analysis and taking x-rays images. The discussion about the success of prototype and measurement results is given in Chapter 6, and finally, the conclusions about thesis work are given in Chapter 7.

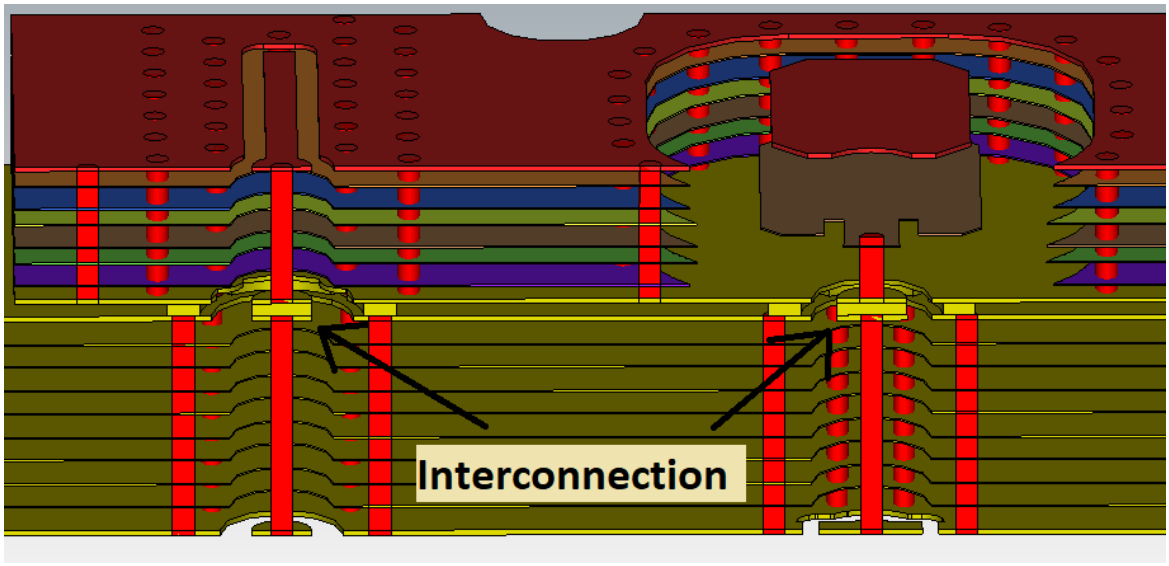

Fig. 1. The interconnection under development.

2 THEORETICAL BACKGROUND

This master's thesis theory part introduces basics and theoretical background needed for this research work and the chapter is divided in two sub-chapters. The first sub-chapter focuses on antenna and its feeding, including microstrip patch antenna, antenna array, RFIC (Radio Frequency Integrated Circuit) and GCPW-line (Grounded Coplanar Waveguide). The second sub-chapter in its turn focuses on broadband impedance matching, including S-parameters and broadband impedance matching.

2.1 Antenna

To receive or transmit radio waves, antennas are used. Every conducting metallic device, with a discontinuity, can be used to radiate electromagnetic waves, if there is alternative current flowing through it. Antennas are especially made for radiating or receiving electromagnetic waves on chosen frequency and bandwidth. Feed is used to connect an antenna to a signal path, for example, a patch antenna to a microstrip transmission line. The antenna is fed with signal having desired amplitude and phase.
To define the antennas radiation properties as a function of space coordinates, radiation pattern is used. Radiation pattern defines antennas' radiation properties in graphical form, for example in two- or three-dimensional representation. In the case of one antenna, the radiation pattern of antenna does not depend on the amplitude and phase. Additionally, if having an array of antennas, the combined radiation pattern depends on the amplitudes and phases fed to antennas. [7]

2.1.1 Microstrip patch antenna

Microstrip patch antennas, usually referred to as patch antennas, defined as an antenna, made from very thin metallic strip, which is placed above the ground plane. Furthermore, substrate (dielectric material) is placed between patch antenna and ground plane. [7]

A patch antenna includes feed between antenna structure and substrate. The patch antenna feed has many configurations, although the most popular ones are microstrip line, aperture coupling, proximity coupling and coaxial probe. Coaxial-line feeding includes inner conductor and outer conductor. In this system, the outer conductor is connected to the ground plane, while the inner conductor is attached to the radiation patch. This type of feed is easy to match, has low spurious radiations outside the system and is also easy to design. The patch antenna model with buried coaxial-line feeding, is illustrated in Fig. 2. In the figure, the substrate is represented with green color, while the patch antenna is seen as red, as well as the ground around the antenna patch. [7]

The maximum radiation of patch antenna can be found pointing straight forward, in normal direction from antenna patch area, when looking from behind of the antenna. A patch antenna can be of any shape; however, circular and rectangular shapes are the most practical. The low cross-polarization is achieved when using a rectangular patch shape. [7]

Patch antennas are inexpensive due to modern printed circuit technology, low profile, simple and can be made in planar or non-planar surfaces. The disadvantages using patch antennas are

poor scan performance, low power, significantly high Q-value, spurious feed radiation and very narrow bandwidth. However, one possibility to increase the bandwidth and efficiency is achieved by increasing the height of the substrate [7] or by placing a second patch antenna in front of the original one [8][9][10]. This setup is called a stacked microstrip patch antenna [8][9][10] and it functions as a normal microstrip antenna, but the lower patch couples electromagnetically to the upper patch [8][10].

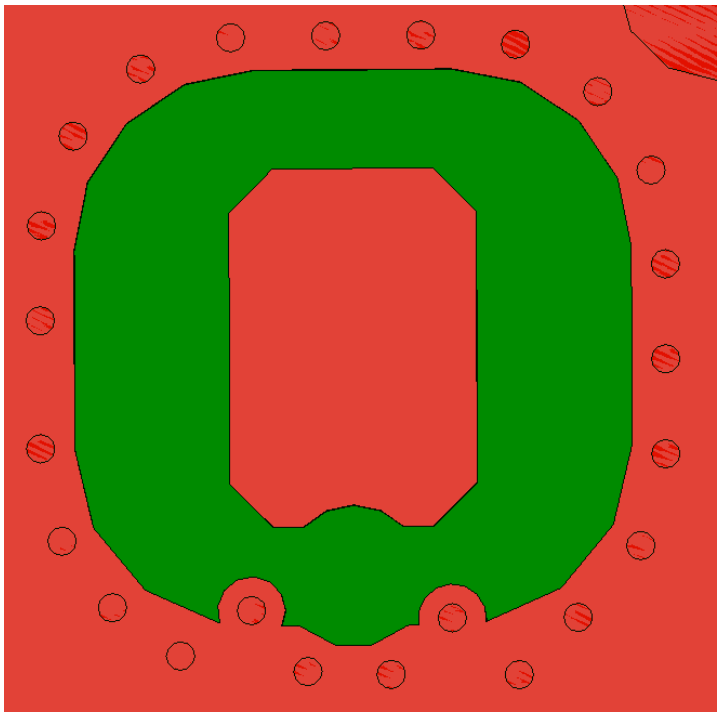

Fig. 2. Microstrip patch antenna on substrate.

2.1.2 Antenna array

In some cases, the characteristics of one antenna are not enough, but an array of them may fulfill the desired characteristics. An antenna array is created by arranging the antenna elements in geometrical shape or array. To illustrate this, a 4x4 element planar array is shown in Fig. 3. In the case of having identical antennas, the radiation pattern can be calculated using the so-called array factor -method. In this method, the electric field of one antenna element is multiplied with an array factor, which considers the number of antennas, the geometrical shape of array, amplitude and phase of each antenna and the progressive phase between antennas. [7]

When using an array of antennas, for example, an array of patch antennas, the radiated beam gets narrower and the gain in the main beam increases [7]. The beam can also be tilted to a desired direction, for example ±40˚ vertically (elevation) or horizontally (azimuth) [5]. In this method, every antenna must be fed with a desired amplitude and phase [7]. To feed the patch antennas in modern antenna arrays, especially in 5G applications [1][3][5], specified integrated circuits for radio frequencies, RFICs, are used.

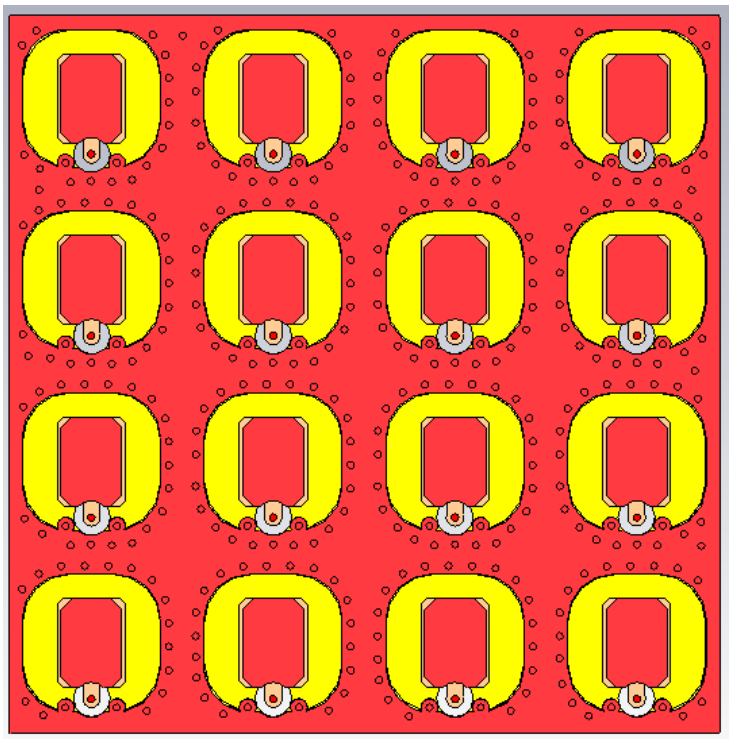

Fig. 3. A 4x4 antenna array of patch antennas (substrates are hidden for visibility).

2.1.3 Radio Frequency Integrated Circuit - RFIC

In modern 5G related implementations, RFICs are used for antenna feeding. One RFIC may operate from one up to sixteen antenna patches, while patches can be dual-polarized, increasing the maximum number of feeds to 32 [1][6]. Generally, RFIC handles TX and RX transmissions and includes digital controls, grounding connections, powering and IF (Intermediate Frequency) and LO (Local Oscillator) signals [2]. In 5G mm-wave applications, RFIC is located as close as possible to the antenna to minimize the system dimensions, and equal-length feeding lines are included to ensure a matched phase response for functional antennas [6].

In the latest technology, the flip-chip RFIC is soldered at the bottom of passive antenna package which is again soldered to the system "motherboard". Using this method, the routing gets easier from RFIC to antenna, while the level of integration increases. In this approach, the interconnection utilizes low frequency, because RFIC includes an integrated mixer that does the downmixing before the signal goes to interconnection. [1]

2.1.4 Grounded Coplanar Waveguide - GCPW

Instead of using RFIC at the bottom of motherboard, grounded coplanar waveguide (GCPW) is used in this thesis for measuring purposes (more in Chapter 4.). The grounded coplanar waveguide consists of a conductor in center, which is considered as a signal conductor, and the ground conductors on both sides of the signal conductor with chosen separation to a signal conductor. These conductors are placed on substrate, while ground plane (another conducting layer) is placed under the substrate.

When dimensioning the GCPW transmission line, the needed parameters are: the width of signal trace W, the width of the separation between signal trace and ground layer horizontally D, thickness of conducting layer T, thickness of substrate, i.e. vertical separation between two conducting layers, H and dielectric constant of substrate ε_r. Using these parameters, the chosen characteristic impedance, Z_0, can be calculated. It is worth mentioning that the characteristic impedance does not depend on the length of GCPW line. The dimensioning for GCPW-lines is carried out in Chapter 4. [11]

2.2 Broadband impedance matching

In microwave design, the idea is to transfer power from one stage to another as efficiently as possible [12]. To achieve the best possible matching or efficiency in the path from GCPW-line to antenna, broadband impedance matching is needed. This sub-chapter introduces the basic principles of S-parameters and broadband impedance.

2.2.1 Scattering parameters

The circuits, devices and systems are modelled using scattering parameters (S-parameters), which are obtained through measurement of power or voltage quantities [12]. In a two-port system, Fig. 4 below, the S-parameters using voltage quantities are found by sending signal from one port and by measuring reflected voltage (the voltage coming back to the same port) or received voltage that propagates to another port. [12]

Scattering parameters, using voltage quantities, are derived from a basic two-port network, shown in Fig. 4. In that figure, input port (port 1) is seen on the left side, output port (port 2) is located on the right side of the two-port system. In port 1, voltage source V_{IN}, is connected in series with resistor R_S. In port 2, only load resistor R_L is connected. Inside both loops, the direction of voltages is illustrated by using arrows and texts for voltages V_{1+}, V_{1-}, V_{2+} and V_{2-}. The voltage V_{1+} is denoted as an incident wave, meaning the wave that is generated in V_{IN}, while V_{1-} is denoted as a wave reflected from two-port system. The voltage at the input is considered as $V_{1+} + V_{1-}$. Respectively, on the output side, V_{2+} denotes the wave reflected from load resistor R_L and V_{2-} denotes the wave going from input to output. [12]

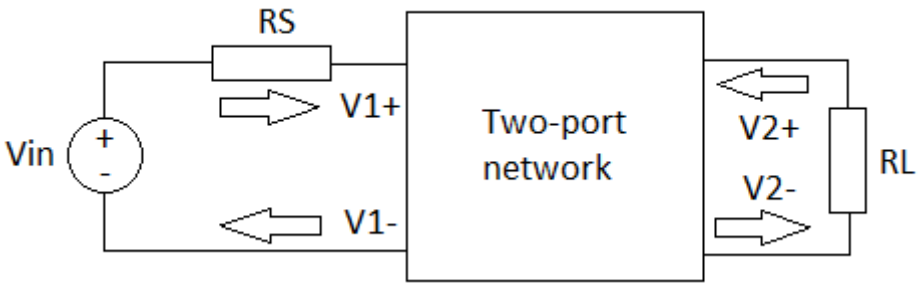

Fig. 4. The basic two-port system illustrating S-parameters.

The actual S-parameters are derived using a two-port network. The S-parameters are given in the form of S_{MN}, where M means the port under measuring, while N means the port that is transmitting. In a two-port system, there are four possible S-parameter combinations: S_{11}, S_{12}, S_{21} and S_{22}. Combining S-parameters and voltages from Fig. 4 above leads to

$$V_1^- = S_{11}V_1^+ + S_{12}V_2^+ \quad (1)$$

$$V_2^- = S_{21}V_1^+ + S_{22}V_2^+. \quad (2)$$

From Eq. (1) and (2), the S-parameters are solved and shown as

$$S_{11} = \frac{V_1^-}{V_1^+}, while\ V_2^+ = 0 \quad (3)$$

$$S_{12} = \frac{V_1^-}{V_2^+}, while\ V_1^+ = 0 \quad (4)$$

$$S_{21} = \frac{V_2^-}{V_1^+}, while\ V_2^+ = 0 \quad (5)$$

$$S_{22} = \frac{V_2^-}{V_2^+}, while\ V_1^+ = 0. \quad (6)$$

The meaning for S-parameters can be seen from Eq. (3)-(6). In Eq. (3), S_{11} means the ratio between reflected wave and incident wave, which is measured from port 1, while reflection from port 2 equals zero. In RF-design, the most commonly used parameter is considered as S_{11} due to its ability of quantifying the accuracy of input impedance matching in the receiver. The S_{12} means the ratio of input port reflected wave to output incident wave, while the input port is fully matched. Measuring S_{12}, one should remember that the signal source is in the output port. The S_{12} is considered as reverse isolation, indicating the level of output signal coupling to input. The S_{21} represents the gain or loss which is achieved from circuit, meaning the ratio between output incident wave going to input, while reflection from port 2 equals zero. The S_{22} measures the ratio between reflected wave and incident wave measured at output, while reflection from port 1 equals zero. Again, for S_{22} parameters, the signal is driven in port 2. [12]

To summarize the S-parameters, S_{11} and S_{22} indicate the matching accuracy in input and output ports, respectively, while S_{12} and S_{21} indicate the gain or loss between ports. For a better illustration of S-parameters, Fig. 5 is presented. In that figure, the arrows represent the direction of signal flow [13]. [12]

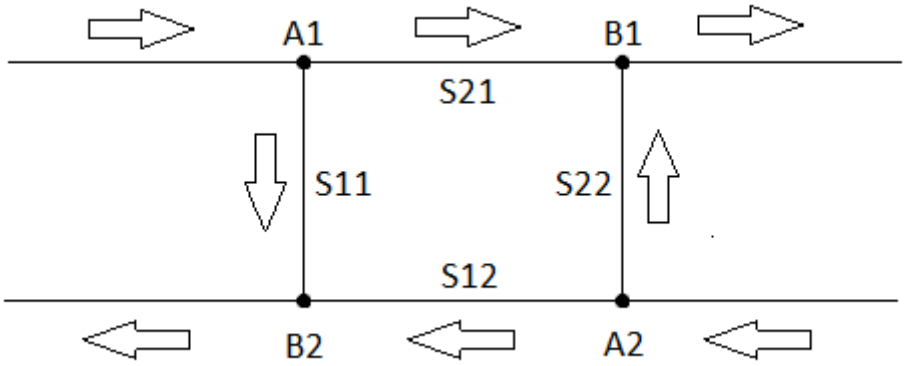

Fig. 5. Illustration of the S-parameters.

Finally, to convert the S-parameters with voltage quantities to the most used unit, decibel [dB], the Eq. (7) is used [12]

$$S_{MN}(dB) = 20\log|S_{MN}|. \tag{7}$$

2.2.2 Broadband impedance matching

When connecting two electronic systems together as efficiently as possible, good impedance matching between systems is needed. An electronic system can be for example antenna, transmission line or component. Every electronic system has its own characteristic impedance, which consists of real part (resistance) and imaginary part (reactance). The characteristic impedance is considered real, if the imaginary part (reactance) equals zero. [13]

In RF-systems, characteristic impedance is normally 50 Ω, which is a trade-off between maximum power capacity and minimum attenuation in coaxial cables. In these cables, impedance of 30 Ω represents maximum power capacity, while minimum attenuation occurs at impedance of 77 Ω. [13]

The characteristic impedance of a system is frequency dependent and Smith diagram visualizes the frequency dependent matching. In the center of Smith's chart, the load is fully matched to reference impedance. At the circumference of chart, the impedance is purely imaginary, while purely real impedances appear on the diagonal of Smith chart. [14]

In addition, other suitable parameter, along the S-parameters, illustrating the matching is so called reflection coefficient

$$\Gamma = \frac{Z_L - Z_0}{Z_L + Z_0}, \tag{8}$$

where Z_L means the characteristic impedance of load, while Z_0 illustrates the reference impedance. The reflection coefficient can have a value between zero to one, while zero means optimal matching and a value of one means that the matching is ended with open load or is short circuited [14]. By choosing the wanted reflection coefficient from the matching point of

view, a circle with a radius of reflection coefficient can be drawn on Smith chart. The impedance matching is satisfied, when the impedance curve stays inside the circle drawn. [15]

Fig. 6. illustrates an example of broadband impedance matching between 26.5 GHz and 29.5 GHz, leading to the band of 3 GHz. The circle is drawn with a chosen reflection coefficient of 0.1, that has been converted to dB measures, using Eq. (7), leading to -20 dB matching. In Fig. 6, optimized vs. non-optimized (default) S_{11} and optimized vs. non-optimized (default) S_{22} are shown in purple, green, red and blue, respectively. As it can be seen from the figure, the non-optimized results are outside the reference circle, while optimized results are just on the circumference of the reference circle. This means that the optimized matching almost satisfies the optimization goal in this example.

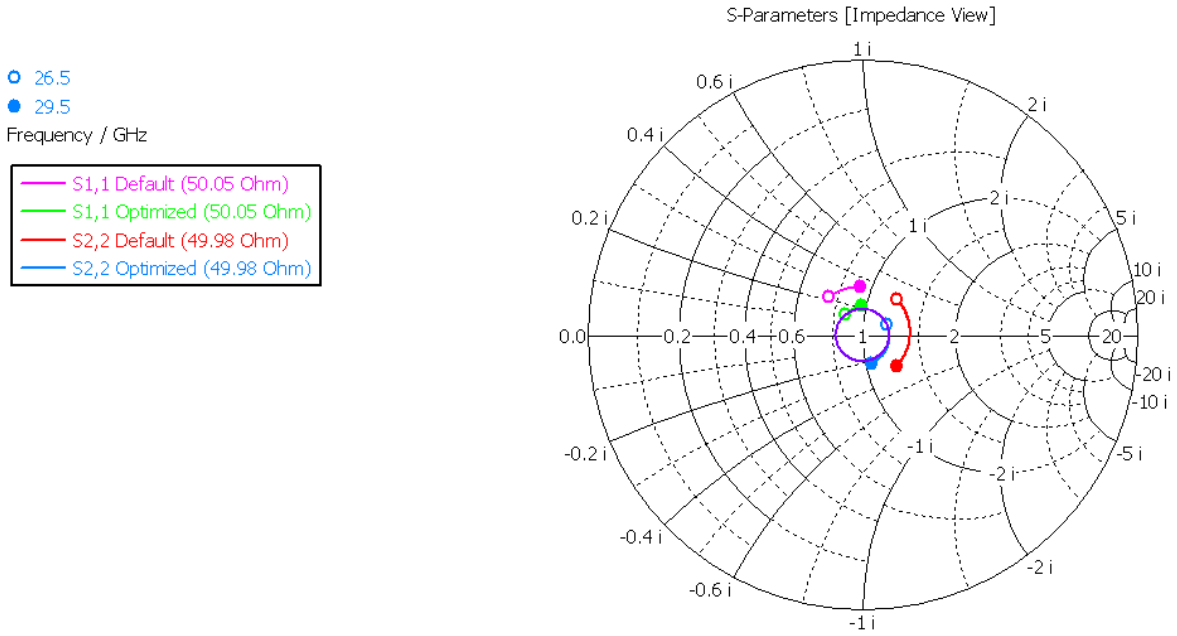

Fig. 6. Broadband impedance matching with a reference circle with -20 dB specification, optimized vs. non-optimized.

3 INTERCONNECTION OPTIONS BETWEEN ANTENNA MODULE AND MOTHERBOARD

The transition between two transmission lines can be implemented by using two different methods. The first method uses electromagnetic coupling between transmission lines. With this approach, the leakage from coupling might lead to unwanted substrate-waves, which can again cause crosstalk to other lines or components leading to functionality problems. To overcome the problematic coupling transition, galvanic connection is introduced. The galvanic connection connects devices vertically to each other, using solder balls, pads, lands or bonding wires, which are connected using vertical via holes. Using galvanic connection, compact size and large bandwidth up to mm-wave frequencies can be obtained. [16]

This chapter introduces different options for galvanic connection between passive antenna matrix and motherboard. The pros, cons and properties of different methods are considered and discussed. The chapter consists of three sub-chapters. The first sub-chapter introduces the machinery soldering process for SMT (Surface Mount Technology), which is eventually needed in every interconnection option. In the first sub-chapter, the possibilities of creating the interconnection by installing the antenna modules on motherboard as surface mountable devices (SMDs). In this approach, the SMD connection methods would be LGA (Land Grid Array) or BGA (Ball Grid Array). The second sub-chapter considers usage of SMD plug-in RF-connectors as an interconnection method. Finally, in the third sub-chapter, usage of SMD antenna array connector is introduced and discussed.

3.1 The antenna modules as Surface Mounted Devices

In this sub-chapter, the basics of the machinery soldering process for SMDs is introduced and different case-types applying to the SMD-method is presented. A known casing method applying to the SMD-method is called the grid array method [17]. In the grid array method, the component has a high number of connections on the underside of the component case [18]. The grid array method includes LGA and BGA, and both are introduced in separate sub-chapters.

3.1.1 Machinery soldering process

In soldering process, the components are categorized roughly in two groups. The first group consists of through hole components, where components “legs” are put through the hole and soldered in. Through hole components are the most traditional ones used. [17]

Newer, a more advanced and more used method, SMD, in which a component has connectors (pads or lands) underside of the case and the same pads or lands on the PWB. The soldering between PWB and the component is done using the so-called reflow soldering-method. The first step is to make a stencil from the PWB layout. A stencil is a plastic or metal plate (more accurately: stainless steel), with holes for applying soldering paste to PWB footprints according to the layout. A stainless steel stencil is illustrated in Fig. 7. In the stencil, the dimensions of aperture must be slightly smaller compared to the footprint to avoid the spreading of soldering paste during reflow. The soldering paste includes usually tin, copper and flux, from which, the flux fades away as a gas. The soldering paste is applied over a stencil, filling the holes. The

amount of soldering paste per hole is controlled by choosing right dimensions and shapes of holes in a stencil, and by choosing the right thickness of a stencil. When using a soldering paste with metal content of 90%, the overall volume after soldering will be about 50% from the original. In other words, if the stencil has thickness of 100 µm, the eventual solder thickness will be about 50 µm. The reason for halved thickness can be found from flux that fades away. The solder paste with 95% metal content would have eventual solder thickness of about 67 µm with the same stencil. [17]

After applying the soldering paste, a stencil is removed, and the soldering paste can be seen on top of pads on PWB, this is illustrated in Fig. 8. Components will be assembled over the soldering paste and after the assembly, the heat is applied as radiation, convection or conduction, making the soldering paste reflow. [17]

The success of the soldering can be estimated by inspecting the soldering. First, if the solder has remained where it is supposed to be, and no open joints are visible, soldering has been successful. Secondly, if any bridges or soldering balls between other pads cannot be seen, soldering has been successful. The third thing to check is whether the SMD components are at the right places or not. Additionally, using X-ray, also the wet quality of soldering paste and the appearance of voids can be seen [18]. [17]

The soldering joint reliability between component and PWB is tested by using temperature cycling, bias temperature humidity, high temperature on load, thermal shock and mechanical bending and flexing. In addition, for consumer devices, a drop test can be used, and it is the most critical test. [17]

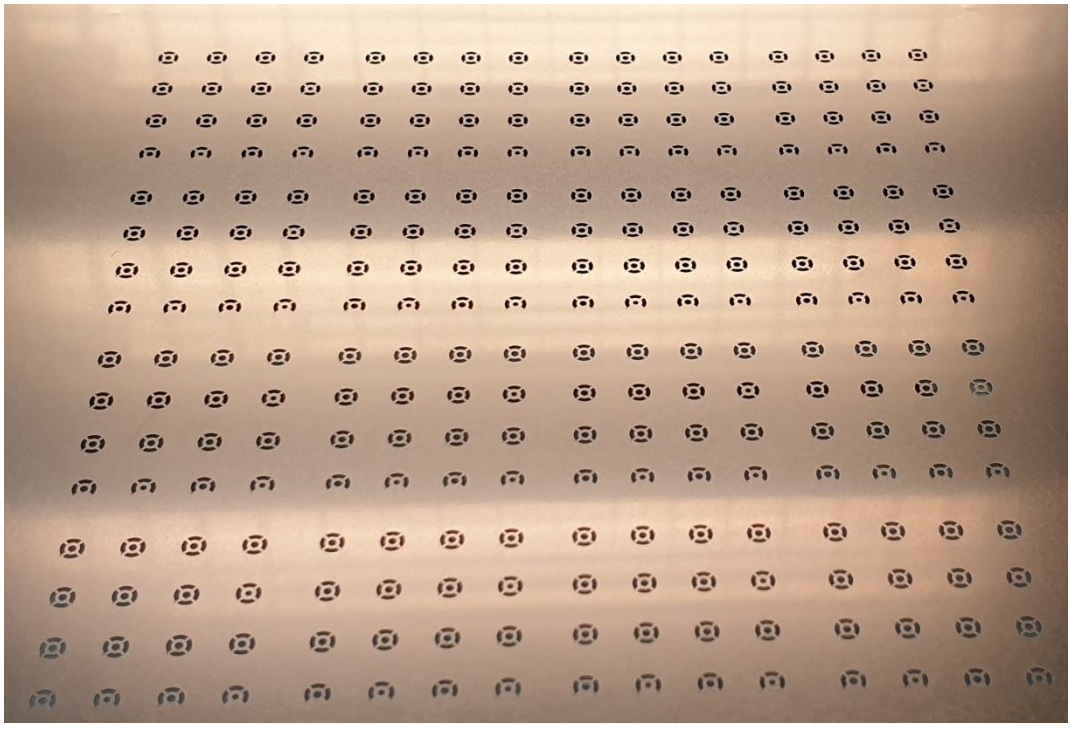

Fig. 7. Metallic soldering stencil (used to solder antenna modules to motherboard).

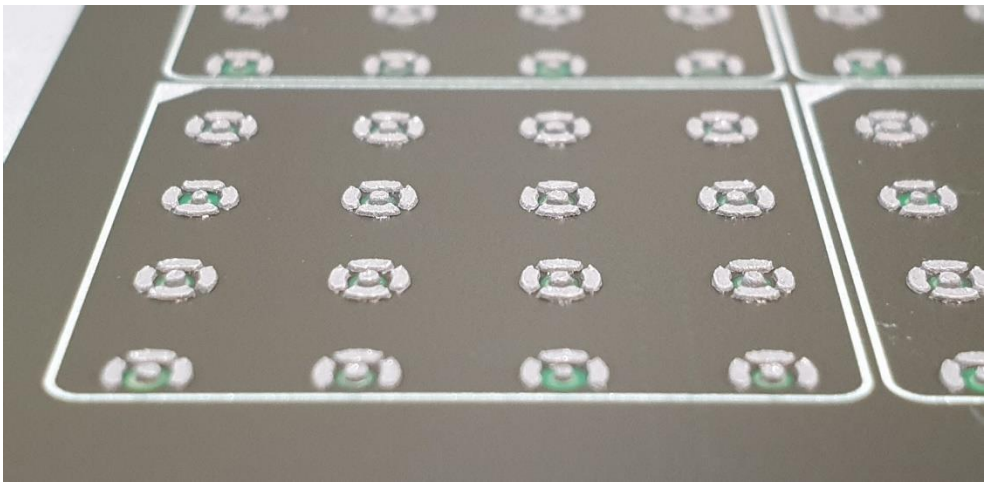

Fig. 8. Soldering paste on the pads after stencil removal.

3.1.2 Land-Grid Array – LGA

LGA belongs to the family of grid array casings. As the name implies, the connection is created using lands or pads on the underside of the component case, as seen in Fig. 9. LGA package type is widely used in consumer electronics due to low profile, low cost and high performance. The low-profile casing is achieved with a lower standoff height, usually 40 µm – 100 µm for a soldering paste due to LGA connection [19]. Lowering the standoff height leads to better electrical performance. However, lowering the standoff height may lead to reliability issues leading to decreased joint robustness. [18]

According to studies related to low profile LGA package soldering, the most critical solder joint can be found from the outermost corners of a large package when doing a drop test. In that outermost corner, the fails occur in interfaces between the solder and PWB pad. To overcome this problem, underfill protection is added between the component and PWB. [18]

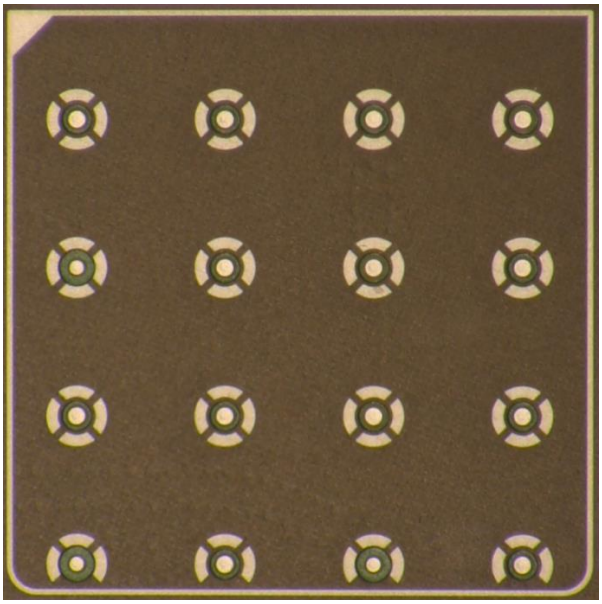

Fig. 9. Land grid array from bottom of the antenna module.

3.1.3 Ball-Grid Array – BGA

To overcome the robustness and void problems with LGA, another grid array method, called BGA, is introduced. In BGA, the lands from LGA are replaced with soldering balls, as seen in Fig. 10 below. Replacing the lands with soldering balls leads to higher standoff, which can be from 80 µm to 300 µm [20]. The BGA method provides better alignment, allows larger tolerance in placement accuracy and, also offers better electrical and thermal advantages, compared to the LGA method. [21]

In more advanced BGA systems, a plastic ball is inserted inside the soldering ball, leading to Plastic Ball Grid Array (PBGA). In PBGA, the spheres underside of component can be made from different materials. These materials can be divided into two groups on higher level: lead-free spheres and lead containing spheres. The manufacturer decides whether they want to use lead-free or not. Anyway, both kinds of spheres have the same function during assembly on PWB. The function of spheres is that they collapse during assembly, and the collapse is controlled by pad geometries and solder surface tension. Using this method, an optimal soldering shape is achieved. [21]

From the thesis point-of-view, the BGA or PBGA method seems the best SMD option for connecting passive antenna matrix PWB to the main board. The advantages of BGA are quick and easy installation at soldering process, while providing a low enough standoff height. Nokia Oulu factory has ability to install the BGA balls to the bottom of antenna module, but that work would be done by hand and it would take a lot of time (the antenna modules would require hundreds of soldering balls). The biggest problem with this kind of antenna module, with BGA, is that the antenna module itself is created on PWB. If it was a cased component, the component manufacturer would install the BGA balls under the component. However, in this case, the antenna modules are ordered from the PCB manufacturer, and according to the manufacturer, they do not have ability to install the BGA balls to PWBs.

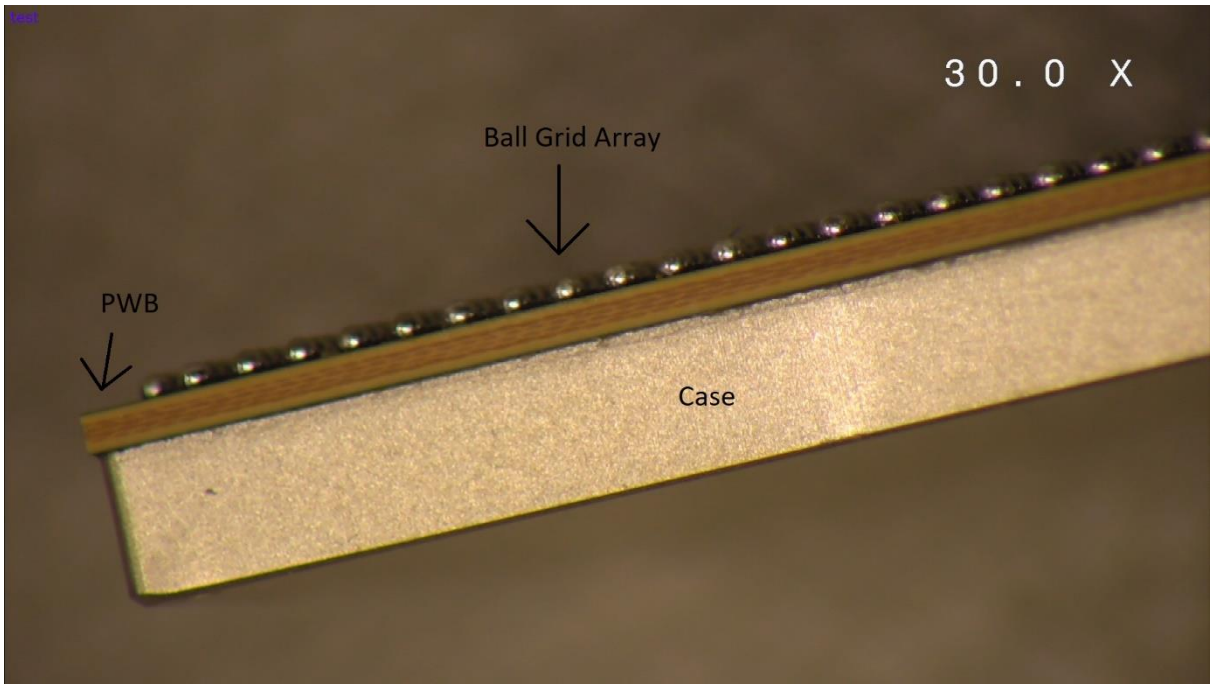

Fig. 10. Sideview of Ball Grid Array.

3.1.4 Comparison between LGA and BGA

The differences between LGA and BGA comes from their properties that are mentioned above. Both options are good and by comparing the positive and negative sides of methods from the thesis point of view, the better option is obtained. The positive sides of using LGA are the lower standoff height, good electrical performance due to a lower standoff height and its overall easy usage. However, the positive sides of BGA are better robustness or reliability with less void problems and faster installation with relaxation of component alignment. They are both extremely low profile compared to other solutions such as an RF-connector.

In this thesis, the LGA connection method is used for the prototype, because the BGA ball insertion should be done by hand and it would require hours of work. Otherwise, BGA would be better and more reliable.

3.2 RF-connector

One method connecting two PWBs together is using SMD RF-connectors and they are widely used in electronic and telecommunication systems for efficiently delivering the signal from one port to another. Different connectors are used for different applications and frequencies. Connectors have male and female parts connected using screw threads or snap-in or plug-in type. For smallest mm-wave approaches, the Snap-on or quick-lock methods are also used, and they provide extremely quick plugging between connectors. To connect an RF-connector to PWB, the flange mount with through holes or SMD RF-connector are used. The flange has usually two or four holes. [22]

From the thesis point of view, the RF-connector must be as low profile as possible, while being able to use snap-in technique. RF-connector must not have threads, because when having

an array of 4x4 antennas they need an equal number of connectors for feeding antennas unique amplitude and phase. This means, that it is not possible to install the antenna module on top of motherboard by connectors using threads because one can only tighten the outer RF-connectors' threads, but not the ones in the inner part. To avoid this problem, snap-in connectors can be used, and the antenna module is only placed on top of the motherboard and pushed a little, to make a connection. The de-attaching is done by simply pulling the antenna module out of motherboard.

However, the usage of RF-connectors is not the optimal solution in terms of integration. To achieve the highest possible level of integration, the distance between antenna module and motherboard must be minimized. The distance between PWBs, i.e. the height of connection, using RF-connectors will be 8.8 mm [23][24], while LGA method gives the maximum of 0.1 mm [19] between PWBs (more in Chapter 4.).

The other considerable thing is the dimension of RF-connector because the distance between antenna elements is fixed to 5.4 mm, from middle of antenna patch to middle of next patch (more in the Chapter 4.). If the RF-connectors are square shaped, the maximum diameter for RF-connector is 5.4 mm to ensure the same electrical length for all patches, in a small passive antenna module. To overcome the dimensioning problem, RF-connector manufacturers have products for mm-wave solutions. These solutions include RF-connectors with a diameter of 4mm [23]. Using these RF-connectors, it is possible to create a connection and it can be easily attached and de-attached. The system includes two similar plugs that are soldered to PWBs and a bullet, which is connected between plugs [23][24].

If the connection was made by using RF-connectors, the last things to consider are the matching, the losses of connector, how the system behaves to external forces and does it require some mechanical solutions to maintain the orthogonality between connectors and antenna module. The connectors are matched to 50 Ω as well as the lines, and the losses are already minimized to as low as possible in manufacturers' design of the connectors, making the losses not that considerable [22]. The ability of maintaining the right position may be possible and at least by using the mechanical solution around the antenna module, the system will be stable and won't move or bend to an angle. However, still the dimensions (i.e. height) of RF-connectors won't change the fact that the connection distance is not optimal, when targeting to the highest possible level of integration, even though it enables attach and de-attach.

3.3 Antenna Array Connector - Molex

The latest interconnection system for mm-wave frequencies is a16-position array connector from Molex, represented in Fig. 11. The connector is designed for mm-wave frequency usage (up to 30 GHz) and it is ideal for connecting two PWBs together by soldering the plug and jack parts to PWBs. The attach / de-attach is made easy and fast because of the plug (or socket) and receptacle parts. The connector can be used in a functional mm-wave product to connect motherboard and antenna part, while enabling easy testing of antenna parts. It is also possible to integrate an antenna inside the plug part in manufacturing process without additional costs. [25][26][27]

The dimensions of connector are 26.16 mm x 26.16 mm for both parts and the overall height of connection, i.e. distance between PWBs, becomes 14.63 mm. According to Molex, the separation between connectors should be at least 10 mm (to de-attach the parts from each other) and the separation between connector pins is set to 5.08mm (calculated at 30 GHz). [25][26][27]

The array connector has few advantages and disadvantages compared to LGA and traditional RF-connector. The array connector enables easier connectivity with fast attach or de-attach. Quick attach and de-attach ease the testing of antenna part. However, the array connector requires more space in all directions, especially in height, i.e. increasing the distance between PWBs. One other thing to consider is that the trend in mm-wave antennas is going towards dual-polarized antennas [3][9][10], but this solution is only functional for a single-polarized system. [25][26][27]

The array connector will possibly be a more cost-efficient solution compared to RF-connectors because one array connector will be much cheaper (according to Molex) than 32 plugs and 16 bullets that are required for traditional RF-connectors. Unfortunately, this 16-position array connector was in a prototyping during this thesis work but can be considered as one possibility for interconnection. Overall, the usage of array connector would be a trade-off between easy connectivity and level of integration due to its measures. [25][26][27]

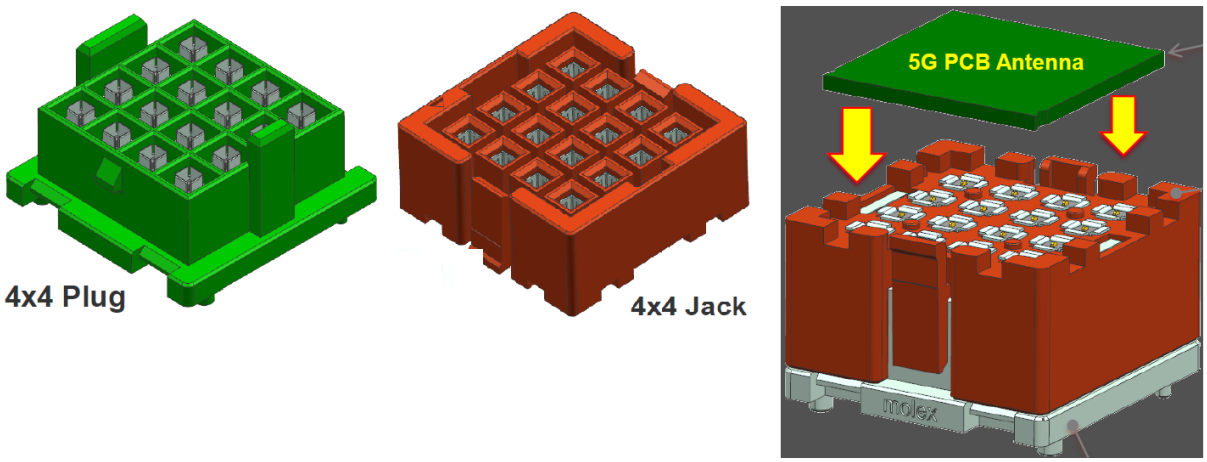

Fig. 11. Molex Array Connector [Molex datasheet with Molex's permission]

4 OPTIMIZING THE CONNECTION

This chapter defines the design process for interconnection and via structure between antenna module and motherboard. The PWB layout designer has designed the antenna module, as well as motherboard, with basic coaxial via structure. The via structure is modified and partly re-designed to prevent the high frequency signal leaking to substrate and to optimize the matching between connections. The design procedure is written in the first sub-chapter, Design, while the optimization part is seen in the second sub-chapter. The final optimization for matching the connection is done by using the modeFRONTIER optimization software, in the third sub-chapter. At the fourth sub-chapter, the optimized solution is converted to layout and its functionality is verified and modifications are done if necessary.

4.1 Design

The system to design includes motherboard and the antenna module. The antenna module will be machinery assembled and soldered to motherboard. One motherboard includes an array of 4x4 antenna modules. To measure the via structure and connection, GCPW-lines are designed to the system, and two different measuring systems are needed. Those systems are GCPW-via-GCPW and GCPW-via-antenna structures. The idea of GCPW-via-GCPW is to measure the whole connection, including matching and losses, from top of antenna module to bottom of motherboard. On the other hand, GCPW-via-antenna structure provides a method to measure matching and antenna radiation pattern. This chapter considers all the steps in design procedure, including sub-chapters of PWB materials and stack-up, GCPW-via-GCPW and GCPW-via-antenna structures, antenna module and motherboard.

4.1.1 PWB materials and stack-up

The PWB materials and stack-up were chosen with a layout designer, and the material of antenna module is especially chosen for mm-wave frequencies, while the motherboard material is specified to the maximum of 10 GHz signals. There is a reason for using the material that is not specified to mm-wave frequencies: to test the function of material on mm-wave frequencies with a material tester on Nokia. The lower frequency material is cheaper compared to higher frequency material, so if the functioning is good enough, the material can be used also for mm-wave frequencies leading to increased cost efficiency.

The material tester itself is based on balanced-type circular resonators having slightly different resonance frequencies due to a different disk radius. Using this setup, relative dielectric constant, ε_r, and dielectric loss tangent, tan δ, can be accurately measured. The structure of the tester, shown in Fig. 12, includes two weighted conductor plates, circular resonator disks and coaxial cable excitations. Two similar sheets of the dielectric material under measurement are set between the circular conductor plates, and the resonator disk is centered between the sample sheets. For measurements, RF-cables are installed between RF-connectors of a network analyzer and the weighted conductor plates. Using this type of material tester, the

resonator fringing effects are corrected, losses from conductors are canceled and multiple frequencies measured simultaneously. [28][29]

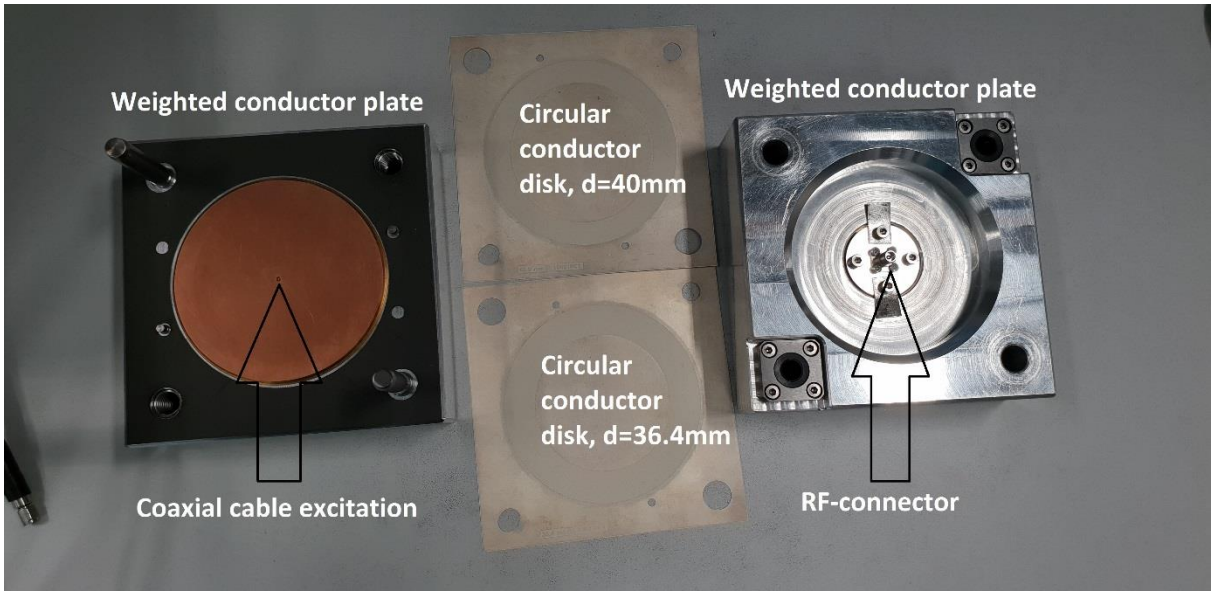

Fig. 12. Material tester setup.

The material tester results are given in Fig. 13. In that figure, the left-hand side shows the measurement results from the dielectric constant measurement while the right-hand side shows the results of the loss tangent measurement. The red lines illustrate constant values of dielectric constant and loss tangent, respectively. The blue spots illustrate measurement results on different frequencies using resonators with a different disk radius. The different disk radius leads to differences between measurement results, as seen on the left side in Fig. 13. According to Fig. 13, the mean value for dielectric constant at 25 GHz is calculated to be 3.7, while the mean value for loss tangent is 0.008. These values are used for motherboard substrates in simulations. The antenna module has a dielectric constant of 3.08 for prepreg layers and 3.34 for core layers, while the loss tangent is 0.002 and 0.0025, at 25 GHz, respectively.

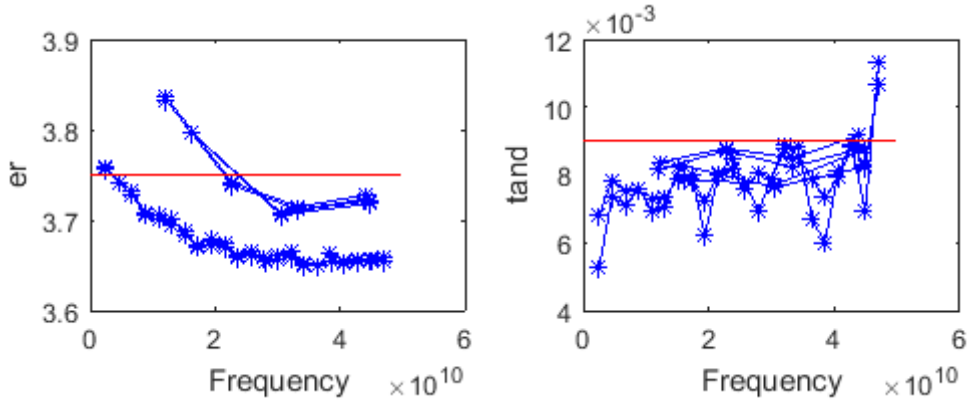

Fig. 13. Measurement results for motherboard dielectric constant and loss tangent.

After choosing the suitable materials for PWBs, PWB stack-ups are constructed, and shown in Fig. 14. The stack-up for the antenna module consists of eight-layer structure that is made

symmetrical around core material in the middle of PWB. The stack-up includes two antenna layers for a stacked microstrip antenna (metal 1 (M1) – parasitic patch, (metal 4 actual patch), one ground / signal layer (metal – 8) and five ground layers (metals – 2,3,5,6,7). These ground layers are needed to provide enough spacing between antenna layers and ground plane. The overall thickness of the antenna module PWB is 1.326 mm. The stack-up for motherboard includes 10-layer structure with two signal / ground layers (metals 1 and 10), while other layers are ground-layers (metals 2-9). The overall thickness of motherboard becomes 2.158 mm. The antenna module was imported in ODB++ (Open Database++) format to CST, while the motherboard had to be created to CST according the stack-up. They both were created for further modification, simulation and optimization.

Fig. 14. Stack-up for antenna module and motherboard.

4.1.2 GCPW-via-GCPW and GCPW-via-antenna

When starting the design procedure, ready antenna structure was given to use. Earlier, that structure was in one PWB and included RFIC at the bottom of PWB, while antennas were located on the top of PWB. In this design, the place for RFIC is replaced with GCPW-lines for measuring with a probe or by using the SMD RF-connector. The overall system includes two configurations: GCPW-via-GCPW and GCPW-via-antenna.

The first configuration is called GCPW-via-GCPW, in which the antenna from the antenna module is replaced with GCPW-line. The GCPW-line was set also at the bottom of

motherboard, creating a controlled measurement line from top to bottom, through via structure. The second configuration, GCPW-via-antenna, includes antenna structure, where the antenna radiation pattern or antenna matching, can be measured.

The GCPW-line has two different types in motherboard side. The first one is about 3.25 mm long, while the length of another one varies on motherboard, depending on from which antenna, from the antenna module, it is connected to. The shorter GCPW-line is made for probe measurement, while longer one is meant to be used with SMD RF-connector. As mentioned in Section 2.1.4, the impedance of GCPW does not depend on the length of the line, meaning that the measurement results should not differ between a short or long line.

When designing the 50 Ω GCPW-lines to antenna module and motherboard, it should be noted that both have slightly different stack-up and material, leading to two different sizes of GCPW-lines. In the case of antenna module GCPW-line width, the measures (Section 2.1.4) are: D = 0.2 mm, T = 0.045 mm, H = 0.14 mm and ε_r = 3.08. The values are taken from PWB stack-up, except the distance between signal and ground trace, D, which is chosen according to measuring the probe pitch and is the same for antenna module and motherboard. Giving these values to GCPW-line solver (Polar Si8000) and impedance of 50 Ω, the solver gives the missing trace width of 0.285 mm. The same dimensioning procedure is used for motherboard with parameters of D = 0.2 mm, T = 0.045 mm, H = 0.226 mm and ε_r = 3.7. The result for trace width in motherboard is 0.383 mm. Using these values, the GCPW-lines are drawn and simulated to verify the right measures. The simulated values for these GCPW-lines are 50.053 Ω and 50.08 Ω, respectively. The antenna module GCPW-line with calculated measures is depicted in Fig. 15. Additionally, the motherboard GCPW-line is too wide for SMD RF-connector [30], meaning that a small thinner extension piece of GCPW-line should be installed at the end of original GCPW-line in motherboard, for measurements. This smaller line is 1 mm long and 0.15 mm wide for both GCPW-via-GCPW and GCPW-via-antenna structures. The small GCPW-line extension with RF-connector model, decreases impedance from 50.08 Ω to 49.71 Ω, which is not a considerably huge change.

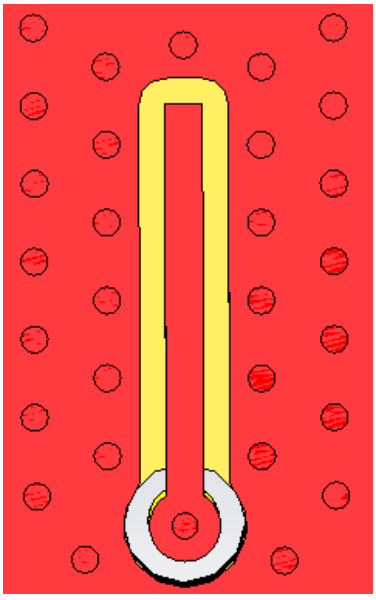

Fig. 15. The antenna module GCPW-line.

4.1.3 Antenna module

The design procedure of antenna module started with a readymade stacked microstrip patch antenna, including coaxial via structure. The antenna element is designed to operate in band of 26.5 GHz – 29.5 GHz, leading to bandwidth of 3 GHz. The antenna element is illustrated in Fig. 16 below, where the parasitic patch is seen as red, while the main patch is seen as light brown and different copper layers are displayed in different colors. The grounding vias (with a diameter of 0.25 mm) are used to connect all copper layers together, providing good grounding around the antenna and around the signal via structure.

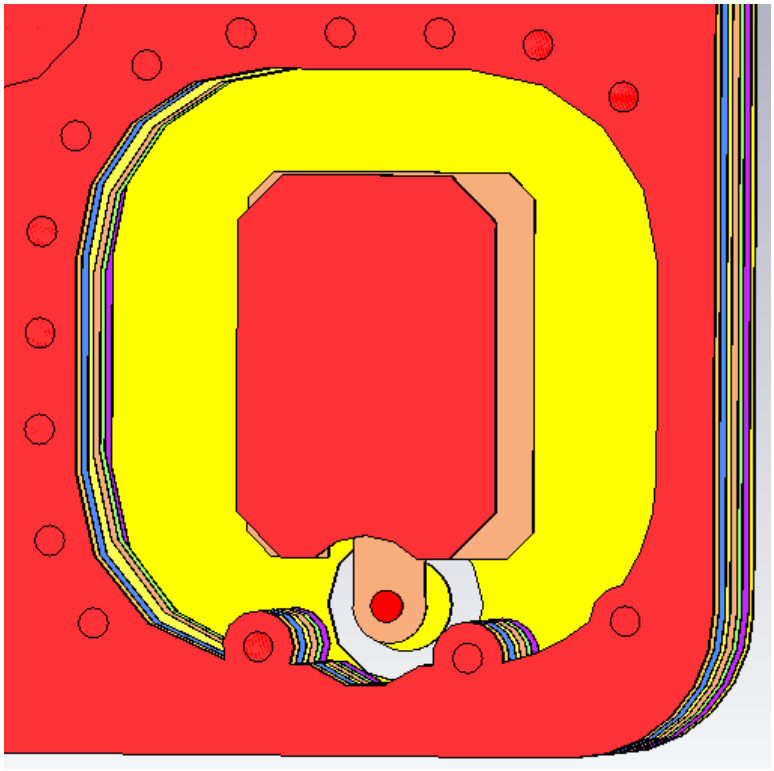

Fig. 16. Structure of one antenna element.

The number of antennas in the antenna module is sixteen, meaning four times four an antenna array. To create such an array, antennas must be separated to constant distance from each other. The separation between antenna elements was set to 5.4 mm, vertically and horizontally, from the patch middle of the patches. The separation equals 0.53 λ at 29.5 GHz and is designed, using basic antenna design rules, by the antenna designer. Using this information, the dimensions of antenna module become 21.6 mm x 21.6 mm x 1.356 mm (height, width, thickness).

Now that the antenna module is considered as an SMT (Surface Mount Technology) component, made from PWB, the separation between antenna modules can't equal zero. There must be a separation between two antenna modules, because the assembling machine requires a gap between components (at least 0.2mm according to Nokia Production). Also, the PWB has some tolerances, meaning that the edges are not strictly straight. To overcome the dimensioning

problem, the dimensions of antenna module decreased to 21.1 mm x 21.1 mm x 1.356 mm, respectively. With this modification, the separation of antennas between two antenna modules kept constant. However, decreasing dimensions of antenna module from its edges, leads to a fitting problem with grounding vias. The grounding vias close to edges were removed and the edges are plated with copper, to ensure good grounding between layers, as well as for the antenna. The antenna element is illustrated in Fig. 16, representing the lower right corner of antenna module, after design modifications are done, and having copper layers installed on left and bottom edges.

At this point, one might conclude that there are no dummy antennas providing the symmetric conditions for all antennas, which is correct. At the start of the design, it was considered to add the dummies around the 16x16 antenna array, but it turned out to be difficult. If these dummy antennas are added to antenna modules, the antenna modules should be 5x5 size and the dummies would be surrounding the 4x4 array. However, in this approach, the antenna array size would increase and the distance from one functional antenna to another, on the next antenna module, would be doubled leading to difficulties with phasing. One other solution would be to create a separate PWB with dummy antennas and assemble it around the 16x16 antenna array, however, this kind of system doesn't sound reasonable. Overall, the additional dummies are dropped from this design for these reasons. After finishing the antenna design, we are now moving on to antenna feeding.

The signal via goes from bottom of the antenna module to roughly halfway of antenna module PWB. The signal via is created all way through PWB in PWB manufacturing process. To get the via only to hallway of antenna module, the unwanted part of via is drilled using a drill with an increased diameter. The increased drilling diameter is used to fully remove the metallization inside the via cylinder. This method is called back drilling and by using this method, the wanted "length" for via can be achieved. Unfortunately, back drilling leaves a small stub (about 0.1 mm) on top of patch antenna, to avoid drilling too deep and breaking the antenna via. The stub itself is problematic because it is metallized and leads to signal reflections [31]. The stub can be seen in Fig. 16 above, where it is located on top of lower antenna patch as a small red cylinder. [32]

At the point, when the antenna module design is ready, the PWB de-paneling must be considered. PWB manufacturers create PWBs in one bigger panel, and the wanted parts are de-paneled from it by using the milling machine. In the PWB panel, there is a gap between wanted PWB parts and the unwanted PWB panel. The wanted PWB parts are connected to the panel from some points by using tabs. In that process, the milling machine cutter, with the same diameter as the gap, follows the gap between PWBs, cutting the connected parts off. [33]

In the case of antenna modules, the antenna module edges are coppered, and the connection parts are at the corners, the cutter must not go through the whole gap. The reason for this is because the coppering on the edges slightly increases the dimensions and the milling machine cutter would remove the copper on the edges. To avoid losing the coppering on edges, the cutter must only cut the corner connecting parts to ensure good grounding for the antenna module.

To prevent antenna modules moving in milling process, three holes with a diameter of 1.5 mm are created to the antenna modules and they are located between antenna elements, as seen in Fig. 17. These holes are needed in the milling machine to avoid the fine movements of

antenna module during milling. The holes also make sure that the antenna module is properly installed, and the patches are facing upwards. Due to the non-symmetric design of the holes, the antenna module only fits to milling machine jig and assembly pallet, antennas facing up. Looking at the antenna module, the lower corners are rounded, while upper corners are sharp and by using this method, for example, the user of assembly machine can be convinced that the antenna modules are set properly to the assembly pallet. Fig. 17 also includes the three GCPW-lines on the antenna module that are used for measuring the whole interconnection from antenna module to motherboard. The antenna under measurement is from the second row and from the third column, marked with a blue rectangle in Fig. 17. This antenna is chosen, because it is surrounded by other antennas, making the surrounding look similar in every direction. These other antennas are referred to as dummy antennas.

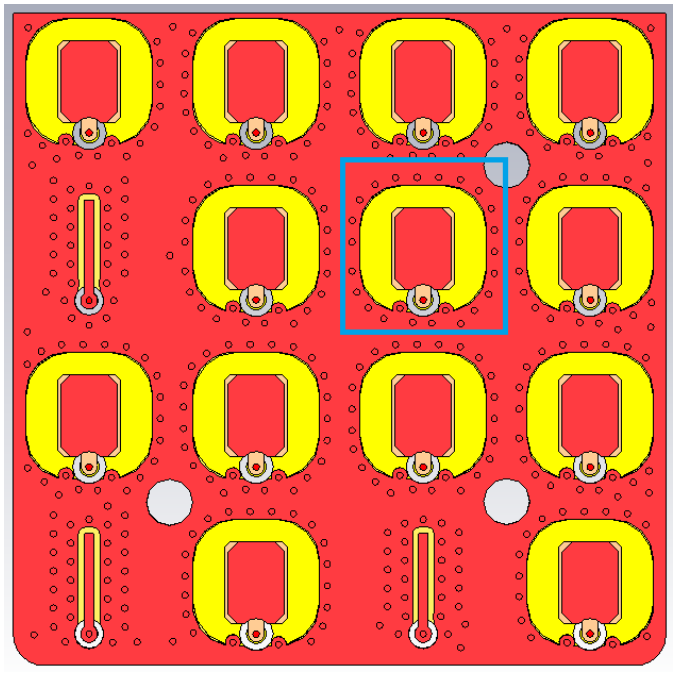

Fig. 17. Antenna module with three GCPW-lines and hold-holes for milling machine.

This antenna module could also be used for Molex antenna array connector (introduced in Section 3.3) after few modifications. These modifications include adjusting the diameter and location of hold-on holes and by adding additional transmission lines to the bottom of antenna module for equal length feeding (the separation of feed is 5.4 mm for the antenna module and 5.08mm for the array connector). After these modifications, the antenna module would fit perfectly on top of the array connector.

4.1.4 Motherboard

The motherboard includes sixteen antenna modules and the overall dimensions of motherboard are 125 mm x 127.1 mm x 2.158 mm (height, width, thickness). The motherboard includes pads for antenna modules and GCPW-lines for measuring purposes. The only components assembled to motherboard are the antenna modules and termination resistors. The SMD RF-connector will

be installed beforehand without soldering and is tightened using screws. The RF-connectors require pads for motherboard and holes for tightening screws [30]. At the bottom of motherboard, there are two different GCPW-lines. These lines are short or long, short lines for probe measurements and longer lines for SMD RF-connector measurements.

As mentioned in Section 4.1.3, the assembly machine requires the minimum of 0.2 mm distance between assembled antenna modules, and the PWB has also its tolerances from cutting or de-paneling. These distances must be considered, when designing the motherboard. As mentioned in Section 4.1.3, the separation between antenna patches must be 5.4 mm sharp. This distance is needed when calculating the positions and separation between antenna module pads on motherboard. The distance from antenna feed of the rightest antenna to the right PWB edge equals to 2.45 mm and the same applies to the leftmost antenna, compared to the left PWB edge. The horizontal separation between antenna modules can be calculated by

$$5.4\ mm - (2 * 2.45\ mm) = 0.5\ mm.$$

Vertically (looking in front of the antenna module), the undermost feed is located 0.895 mm from the undermost PWB edge, while the uppermost feed is located 4.005 mm from the uppermost PWB edge. The vertical separation between the antenna modules on motherboard can be calculated as

$$5.4\ mm - 4.005\ mm - 0.895\ mm = 0.5\ mm.$$

Using these separation values, the antenna modules can be installed on motherboard without a problem with PWB tolerances and antenna separation.

Probably, the most important thing to consider in motherboard design is to terminate the un-used ports to 50 Ω. When measuring GCPW structure or antenna S-parameters, the surrounding ports must be terminated to 50 Ω, to ensure they have no effect on the structure under measurement. If they are not terminated, they are considered as floating ports and most probably influences antennas S-parameters. The used resistors are functional on the frequency range between 26.5 GHz and 29.5 GHz and the 50 Ω termination can be implemented by using two 100 Ω resistors in parallel and connecting desired port between the resistors.

4.1.5 Soldering between antenna module and motherboard

The coaxial via structure comes from the antenna module and continues to motherboard, after the interconnection. The only discontinuity in the whole via structure comes from the soldering pads between signal vias because the diameter of pad is much larger compared to signal via. The circular pads, for RF-signal, are chosen to be the same size for both, antenna module and motherboard, meaning that the soldering paste should be shaped with the same diameter as pads (in simulations). The grounding vias are set around the signal via with a chosen diameter and angle in PWBs. These grounding vias positions are matched in the antenna module and motherboard, to ensure continuous via structure.

The soldering around signal for grounding is done using a sectorized cylinder. The cylinder has outer radius of 0.95 mm and inner radius of 0.65 mm. The cylinder is divided into four equal sectors, that are slightly shortened from end faces, to provide enough space for soldering gases to escape. The actual separation between cylinder sector faces is set to 0.2 mm, while the recommendation from PWB manufacturer was said to be 0.15 mm. The separation is increased, because, in this case, there is also the signal via that emits soldering gases. The overall coaxial-shaped soldering, made by using sectors, is depicted in Fig. 18. The bottom most sector (from Fig. 18.) is removed from antenna modules' bottom most row, because the PWB edge is too close, the removed sector can be seen in Fig. 19. The via functioning was verified with and without the bottom most sector and no effects were found.

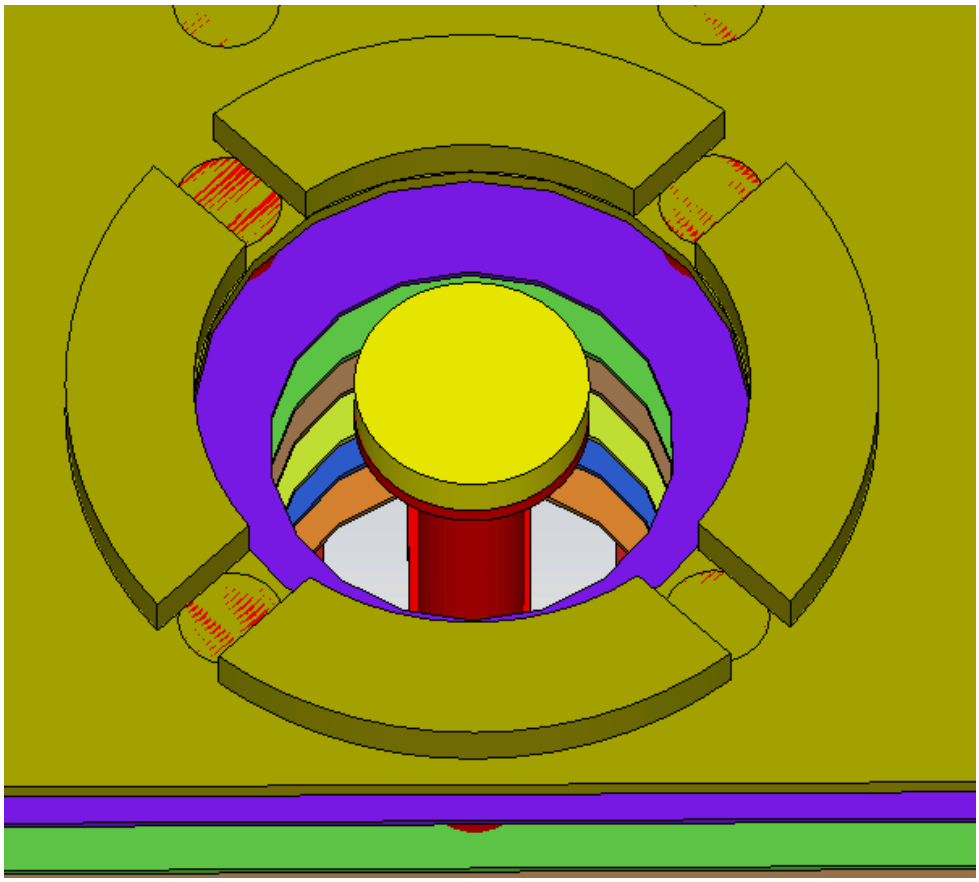

Fig. 18. Soldering under one antenna element (signal + ground sectors).

4.2 Optimization using CST

After the antenna module and motherboard are designed, both the connection and antenna must be optimized for better matching. The optimization is done separately to GCPW-via-GCPW structure, as well as GCPW-via-antenna structure. In GCPW-via-GCPW, the optimization is done using waveguide ports at the end of GCPW-line. The dimensions for waveguide ports are calculated using a macro solver for waveguide ports in CST. When optimizing a two-port system, the optimization considers the matching in each port, as well as losses between ports. On the other hand, when optimizing the GCPW-via-antenna structure, only one port was used, leading to input matching (S_{11}) and the antenna radiation pattern can be measured.

For the optimization goals, the matching (S_{11} and S_{22}) was given to be below -20 dB in the frequency band of 26.5 GHz – 29.5 GHz, for GCPW-via-GCPW. More accurately, for GCPW-via-GCPW, the target was to achieve matching of -20 dB, between 10 GHz to 30 GHz, while the maximum allowed loss (S_{12} and S_{21}) is -1 dB. However, in the case of GCPW-via-antenna, there is only S_{11} parameter to measure and for an antenna, -10 dB in 3 GHz bandwidth is enough.

When starting the design process, the signal via components had to be removed, re-created and parametrized, to change the dimensions of those components, for optimization work. Additionally, the via openings in copper layers were also re-created and parametrized. The optimization process is done by using the parameter sweep option in CST.

4.2.1 GCPW-via-GCPW optimization

The optimization procedure for GCPW-via-GCPW started by choosing one antenna from an antenna array for faster simulations. The left and right bottom corners, in the antenna module, are considered as “weakest” antennas because of that PWB size reduction from two sides and the feed is close to PWB edge leading to a reduced grounding around signal via. Using this knowledge, the chosen antenna is from the bottom left corner of antenna module. However, the antenna structure is removed and replaced by GCPW-line for GCPW-via-GCPW structure.

For the optimization process, there are three main variables in connection that have effects on matching. These variables are illustrated in Fig. 19 below. In Fig. 19, the yellow parts are copper layers, the red cylinder in the middle illustrates the signal via structure with yellow copper soldering between pads (copper used in CST). Around the signal, there are grounding vias seen as red cylinders. The first variable is the diameter of opening around signal via and its default value was 1.1 mm, as seen in Fig. 19. In this GCPW-via-GCPW, changing the diameter of via opening, the diameter or opening changes in every layer. The second parameter is the diameter for pad and soldering paste, and the default diameter for them is 0.5 mm. As mentioned in Section 3.1.1, the diameter of soldering is set a little smaller than it should be but in simulations, they are kept the same. The last, third, parameter is the thickness of solder paste, i.e. the distance between PWBs and the default value for it is 0.1mm, which is the upper limit for LGA soldering with basic methods.

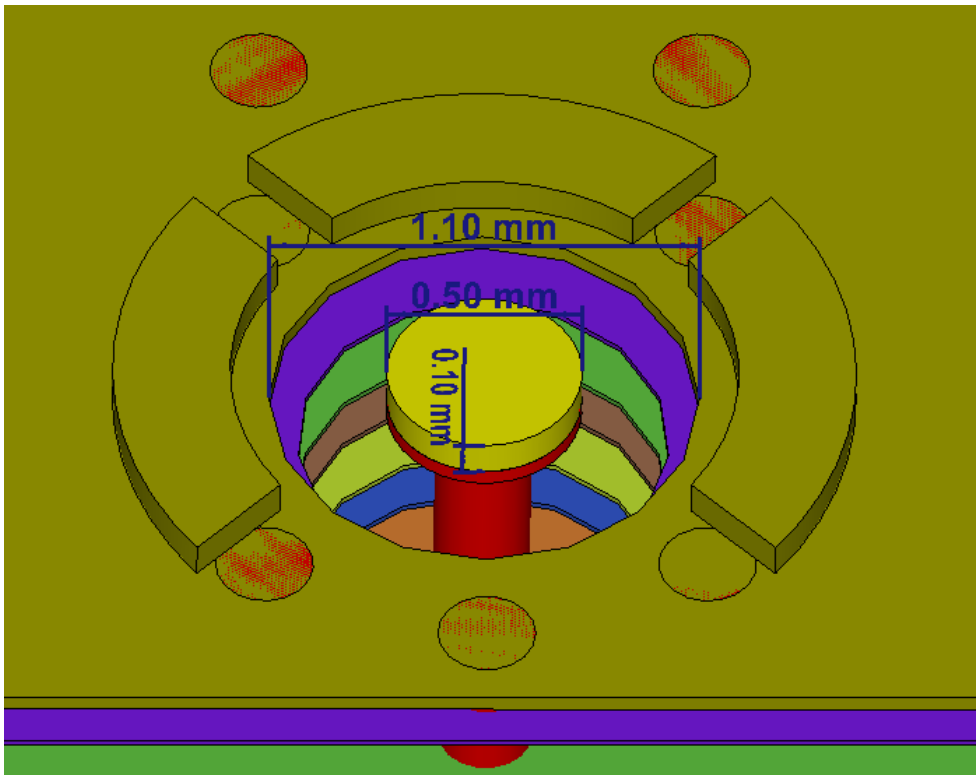

Fig. 19. Visualization for parameters to modify.

Using the waveguide ports at the end of both GCPW-lines, the system is simulated and S-parameters for default values obtained from the frequency band of 10 GHz – 40 GHz. After obtaining the results using the default values, the parameter sweeping started. The first parameter to sweep was the signal pad radius, including the radius of solder paste. The sweep is done with a diameter from 0.55 mm to 0.70 mm and the best results were found near the lower limit, leading to a diameter of 0.55 mm for signal pads and soldering paste.

The next parameter to sweep was the height of soldering paste between pads. The default value for soldering height was set to 100 µm, which is maximum for LGA soldering. The parameter sweep was done between 60 µm and 150 µm. The sweep results indicated that the optimal soldering height for that setup was 100 µm, which was the default value. Using that value, the next sweep was with ground opening around signal via. The default value for ground opening was 1.1 mm as a diameter, while the maximum diameter was set to 1.3 mm. The lower limit is only limited by pitch between signal via and copper layers, which is set to 0.2 mm, leading to a lower limit of 0.95 mm. Using these limits for the ground opening sweep, the results indicated that the optimal opening was with a diameter of 0.95 mm.

To summarize the first parameter-sweeps, the signal pad diameter increased from 0.5 mm to 0.55 mm, soldering height kept at 100 µm and the ground opening around signal decreased from 1.1 mm to 0.95 mm. After the first round, the parameters re-swept, using the same limits, by starting from the signal pad diameter. The pad diameter sweep indicated that the 0.55 mm pad is the best option and by reducing the size, the matching increases. However, according to the layout designer, the minimum pad size with used processes is 0.55 mm (plugged via). Using the same pad diameter, the soldering height sweep was done again, and according to results,

the matching is good at 100 µm, but it gets better when increasing the soldering height up to 150 µm. In this point, it is worth mentioning that the soldering height will be limited by structure, giving a lower soldering height (GCPW-via-GCPW against GCPW-via-antenna).

The problem with the 150 µm soldering height is, however, that the maximum LGA connection height is about 100 µm, and on that height, the matching is good enough, but with 150 µm, it would be almost -3 dB better at the band of 26.5 GHz – 29.5 GHz. One possibility to increase the soldering height is to apply soldering paste at the bottom of antenna modules, when they are still in the PWB panel and then reflow it. After that, the antenna modules are severed from the PWB panel and the edges are refined. Then, soldering paste is applied to motherboard and the antenna modules can be assembled and the system taken to reflow. After reflowing the joint again, the soldering joint height is supposed to increase because the additional soldering paste from the antenna module bumps reforms with the current one. Using this method, a higher soldering height can be achieved and 150 µm soldering height may be possible to achieve. [34][35]

After the modification in soldering height, the ground opening around via re-swept to make sure the connection is optimized. The parameter sweep indicated that the ground opening has no effect anymore. Furthermore, one method that can increase the performance is to change the diameter of opening areas around the signal, in different layers, to achieve better matching and the method is called continuous tapering [36]. The method is applied to this design by changing the diameter of opening on layers with GCPW-line. Using this method, the opening around motherboard GCPW-via structure swept from 0.95 mm to 1.3 mm and the results indicate that the optimal opening diameter is 1.13 mm. In the antenna module side, the matching is better with opening of 0.95 mm. It was worth testing if the same diameter change has effect on layers with soldering pads, this was tested by sweeping those openings from 0.95 mm to 1.3 mm. The sweep shows that by increasing the diameter opening from 0.95 mm to 1.3 mm around the solder pads, gives additional -3.5 dB to matching in band, while losses decrease by 0.05 dB (26.5 GHz) and 0.08 dB (29.5 GHz). The overall parameters are: soldering height 150 µm, soldering pad diameter 0.55 mm, and the diameter of opening around the signal via 0.95 mm, except around the soldering pads 1.3 mm, and opening around motherboard GCPW-line with a diameter of 1.13 mm.

Fig. 20 illustrates the default S_{11} and S_{22} matching against optimized S_{11} and S_{22} in the band of 10 GHz – 40 GHz. In Fig. 20, the non-optimized (default) and optimized values for S_{11}, and non-optimized and optimized values for S_{22}, are illustrated as purple, red, green and blue lines, respectively. Looking at Fig. 20, a few conclusions can be drawn. First, the matching seems to be better with default values from 10 GHz to about 14 GHz, but after that, the optimized matching is better. The optimization increased the matching of port about by 3.5 dB or more, between 20 GHz and 30 GHz. However, the most interesting band is 26.5 GHz – 29.5 GHz, where the improvement is between 4.5 dB to 5 dB. The set optimization goal, -20 dB, is not totally reached between 10 GHz to 30 GHz, but the matching is not far from that.

The losses (S_{12} and S_{21}) of GCPW-via-GCPW-structure non-optimized and optimized solutions are shown in Fig. 21. In that figure, colors brown, green, black and blue, illustrate the non-optimized S_{12}, optimized S_{12}, non-optimized S_{21} and optimized S_{21}, respectively. As seen, the losses of S_{12} and S_{21} are equal, leading to only two visible traces, black and blue. From Fig.

21 we can see that the non-optimized losses seem to have better performance between 10 GHz – 15 GHz, but after that, the optimized ones perform even better. The maximum loss at the end of the band (at 30 GHz) is -0.68 dB, leading to a satisfied optimization result.

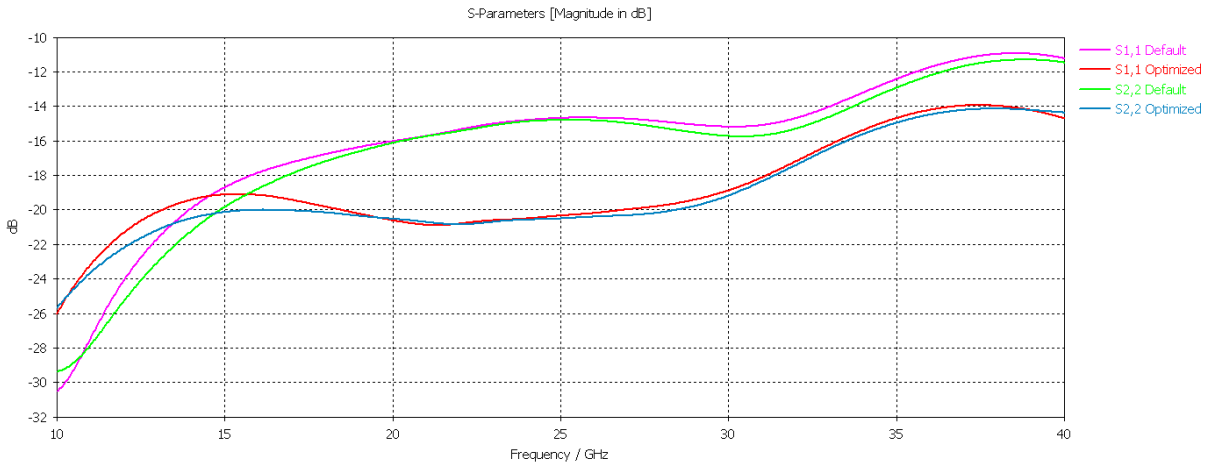

Fig. 20. Optimized vs. non-optimized S_{11} and S_{22}.

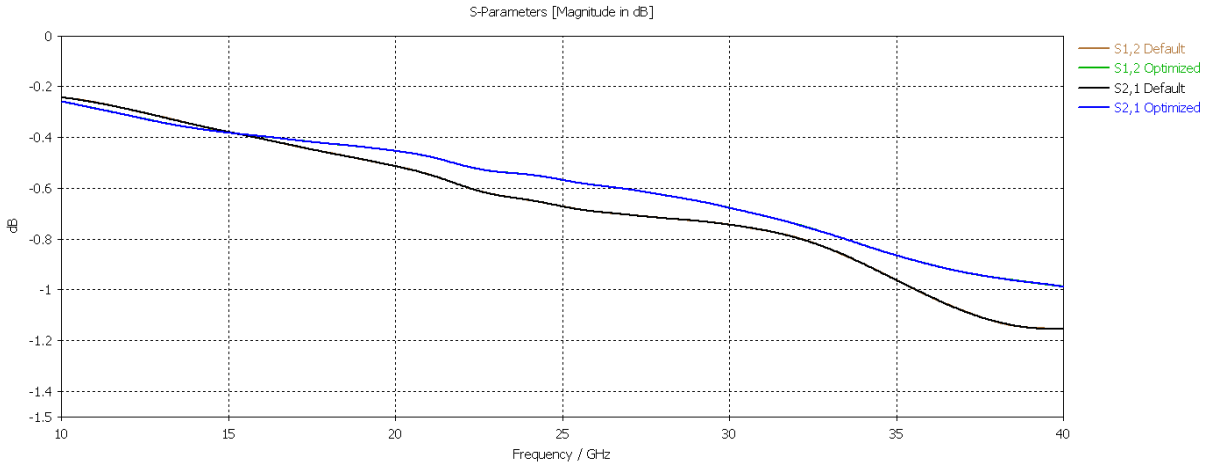

Fig. 21. Optimized vs. non-optimized S_{12} and S_{21}.

The optimization for GCPW-via-GCPW was almost successful when keeping in mind that the optimization target was set to -20 dB. However, the S_{11} optimized result crosses slightly the -20 dB line between 16 GHz to 22.5 GHz and slightly on 26.5 GHz – 29.5 GHz band, making the results considerably good. Using this setup and these optimization parameters, there was no need for further optimization with modeFRONTIER-optimization software.

4.2.2 GCPW-via-antenna optimization

This structure, under optimization, includes the same parameters, with GCPW-via-GCPW structure, represented in Fig. 19. Also, the default values are the same for both structures. The antenna under simulation and optimization is the one highlighted in Fig. 17, because it is

surrounded by other antennas to maintain symmetric surrounding. Before the optimization, S_{11}-parameters of antenna structure were simulated. The results indicate that the antenna functions badly and the resonance frequency is shifted to 26.5 GHz, instead of 28 GHz. and there is an alternative narrow resonance spike at 35 GHz. The malfunctioning of antenna probably comes from the changed antenna stack-up and possibly the airgap between PWBs has some effects on antenna performance as well.

The optimization started by doing parameter sweeping, and the first parameter under sweeping was the diameter of soldering pad with a diameter from 0.55 mm to 0.7 mm. The sweep results indicated that the best results are achieved using the diameter of 0.6 mm. The next modification was to the opening around the signal via and the opening was swept from 0.9 mm to 1.3 mm. According to results, the optimal value was close to 1.2 mm, which was chosen. The last parameter to sweep was the soldering height and it was swept from 60 µm to 150 µm, as in GCPW-via-GCPW. The distance between PWBs, i.e. soldering height, is optimal at 130 µm. As mentioned with the discussion about GCPW-via-GCPW, a smaller soldering height value between GCPW-via-GCPW and GCPW-via-antenna determines the overall soldering height for both structures.

The sweeps were re-done but there was no effect on optimization results. It was also tested to change the openings around GCPW-line or next to the solder pads, with only a small change which was basically negligible. The resulting non-optimized versus optimized S_{11}-parameters, from this optimization, are depicted in Fig. 22. The hand-optimized antenna fits inside the chosen bandwidth, but the deepest resonance is a little bit shifted towards the higher frequencies. The matching values for lower and higher frequency boundaries are -7.83 dB and -11.99 dB, respectively. The final parameters after this optimization for GCPW-via-antenna structure are the following: solder pad diameter – 0.6 mm, soldering height – 130 µm and the opening around signal – 1.2 mm. To improve the matching for GCPW-via-antenna, modeFRONTIER optimization software can be used.

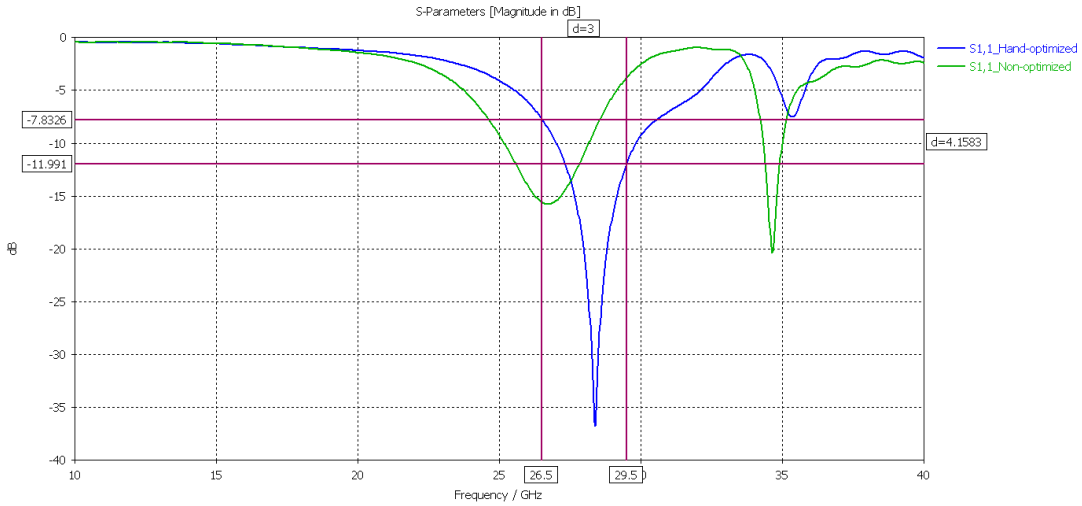

Fig. 22. Non-optimized vs. hand-optimized S_{11}-parameters from GCPW-via-antenna.

4.3 Optimization using modeFRONTIER optimizing software

As mentioned above, further optimization can be done by using optimization algorithms. The advantage of optimization software or algorithms comes from its ability to find a global optimum instead of a local optimum. When doing the optimization by "hand", the local optimum is found first, and after the local optimum, the results start to decrease, meaning that the optimum is found, and the user is fooled by the results. However, the optimization software goes beyond the local optimum and finds the global optimum, which is usually better than local optimum. [37]

One software for optimization is called modeFRONTIER and the algorithm used for optimization in modeFRONTIER is called Multi-Objective Genetic Algorithm – MOGA. For the optimization task, modeFRONTIER uses CST-simulation model, exports its results (S-parameters), reads the results and compares them to optimization goals that are defined. [38]

As mentioned before, the optimization for GCPW-via-GCPW was successful enough without optimization software. However, the GCPW-via-antenna structure optimization was a bit harder and needed some further optimization with this tool. In this optimization for GCPW-via-antenna structure, the same parameters and limits for parameters were used as in Section 4.2.2. The parameters with limits are set to software, the model is uploaded, and the simulation settings are set. The software was set to stop after 55 found solutions and when the goal is reached, it will sort the solutions from best to worst. From these results, eleven best combinations are shown in Table 1, where S_{11}_max (dB) illustrates the S_{11}-value, from inferior frequency boundary, which happens to be 26.5 GHz. As can be seen from Table 1, the performance of antenna structure is just at the level of -10 dB and by using these parameters, the optimization goal can be reached. The S_{11}-parameters illustrating the best optimization result (result 1. from Table 1.) versus non-optimized system, can be seen in Fig. 23.

Table 1. Optimization combinations for GCPW-via-antenna

Result	S_{11}_max [dB]	Solder pad diameter [mm]	Soldering height [mm]	Opening diameter [mm]
1	-10.169	0.64	0.12	1.10
2	-10.096	0.64	0.12	1.08
3	-10.095	0.60	0.12	1.10
4	-10.079	0.64	0.12	1.07
5	-10.034	0.64	0.12	1.06
6	-9.9953	0.64	0.12	1.05
7	-9.8909	0.64	0.12	1.02
8	-9.3866	0.70	0.13	1.10
9	-9.2867	0.70	0.12	1.10
10	-9.0015	0.70	0.12	1.07
11	-8.8092	0.40	0.12	0.80

In Fig. 23, the red line illustrates the non-optimized functioning of GCPW-via-antenna structure, while the blue line illustrates the optimized behavior of the structure. Purple measurement lines are set to illustrate the band between 26.5 GHz and 29.5 GHz, and the S_{11}-

values for optimized solution. These values are -10.021 dB on lower frequency boundary and -11.341 dB on higher frequency boundary and the performance is close to what is shown in Table 1.

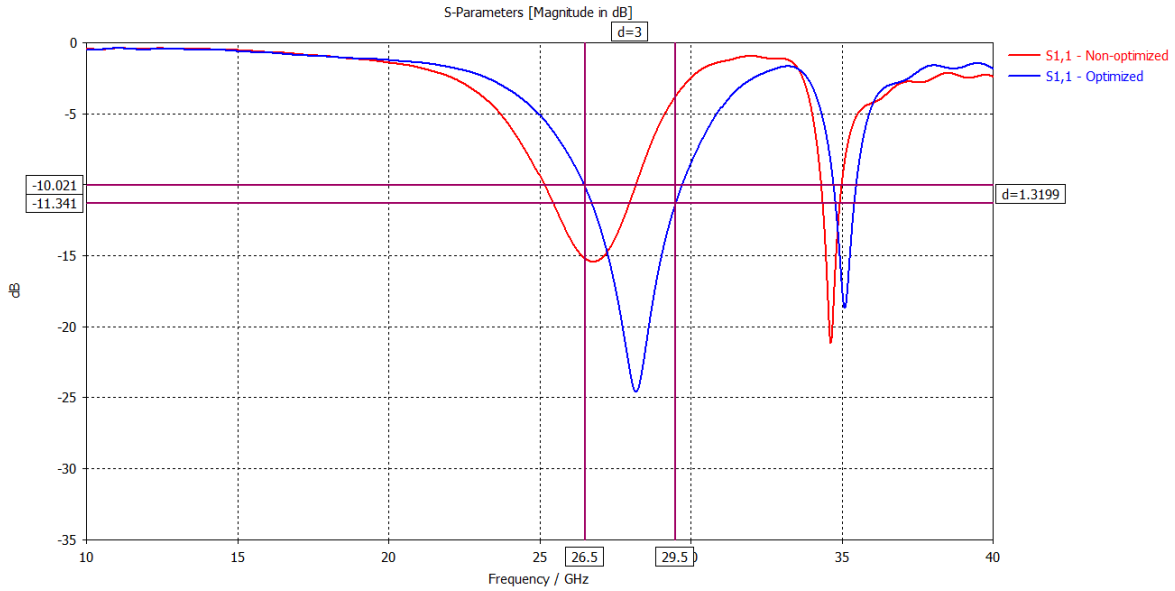

Fig. 23. Non-optimized vs. modeFRONTIER optimized S_{11} results.

However, the method to vary the openings around signal in different layers was not included in the optimization model used in modeFRONTIER. The effects of this method were tested by hand and they had some effects on matching. First, the opening around motherboard GCPW-line was swept from 0.9 mm to 1.3 mm and the results show that the opening of 1.3 mm gives better matching. The next opening sweep to test was the opening around the soldering, meaning the downmost layer from the antenna module and upmost layer from motherboard and it was done with the same parameters as earlier ones. Unfortunately, this opening did not have positive effect on matching and the original value, 1.1 mm, is kept. The difference between modeFRONTIER optimized and opening changed model is depicted in Fig. 24. In the figure, the red line illustrates the modeFRONTIER optimized solution, while the purple line illustrates the one with opening changed from motherboard GCPW-line layer from 1.1 mm to 1.3 mm. The opening-optimized version improves the matching -0.64 dB at the lower frequency boundary, while the higher frequency boundary matching increases -2.45 dB. Finally, after the optimization, the matching at the lower frequency boundary becomes -10.66 dB and on the higher frequency boundary it is -13.79 dB.

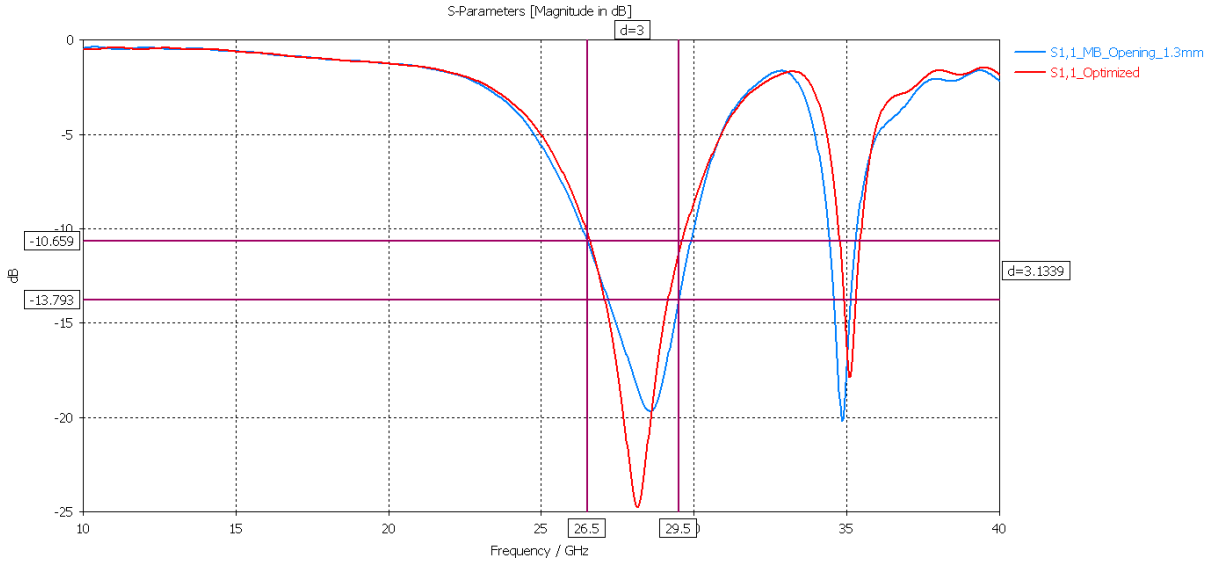

Fig. 24. S_{11}-parameter from modeFRONTIER optimized vs. opening changes.

Overall, the optimization using modeFRONTIER was successful and the results are satisfying. The final parameters after this optimization for GCPW-via-antenna structure are the following: solder pad diameter – 0.64 mm, soldering height – 120 µm and the opening around signal – 1.1 mm, except the around on the motherboard bottom layer around GCPW-line – 1.3 mm. These optimized parameters are used for the final layout model and later, the measurement results from the final layout model are compared with optimized results.

4.4 Test with final layout

After the design and optimization of GCPW-via-GCPW and GCPW-via-antenna structures, the design modifications were made to the layout, by the layout designer, with given measures. The motherboard layout was self-made in CST according to stack-up, and at this point, it was created to the layout. After the layout (from the layout designer) was converted to CST, the functionality of both structures was verified by simulating them.

The simulation results with comparison to optimized results are shown in Fig. 25 and Fig. 26. Fig. 25 illustrates the difference between optimized results and the final layout for GCPW-via-GCPW, while the results for GCPW-via-antenna are shown in Fig. 26. According to these figures, the GCPW-via-GCPW performance degrades about 8 dB at the desired frequency band. In Fig. 26, the maximum resonance of the GCPW-via-antenna structure has decreased from 28 GHz to 26.5 GHz, ruining the matching on the frequency band. Obviously, something has changed between these designs, when looking at the comparison of results.

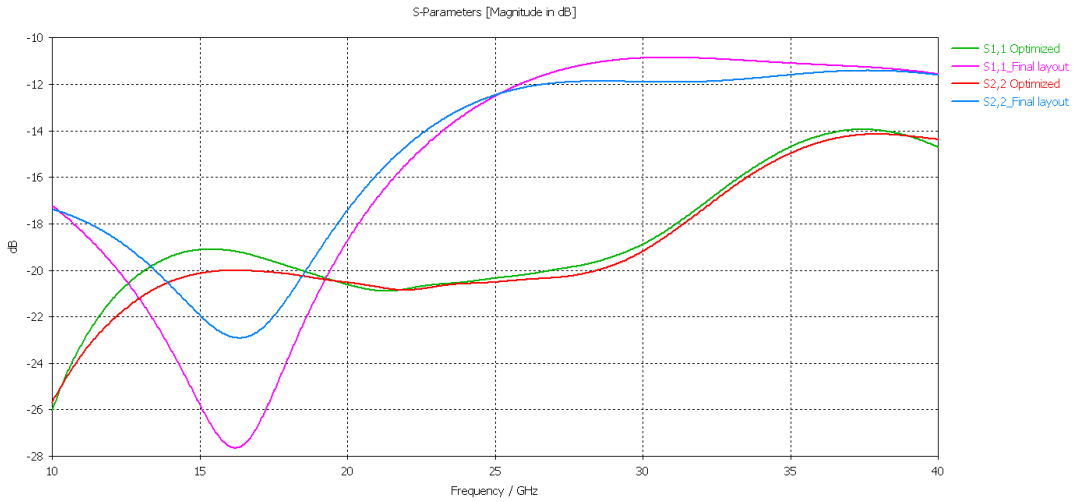

Fig. 25. S_{11} and S_{22} simulation results for GCPW-via-GCPW structure - optimized vs. final layout.

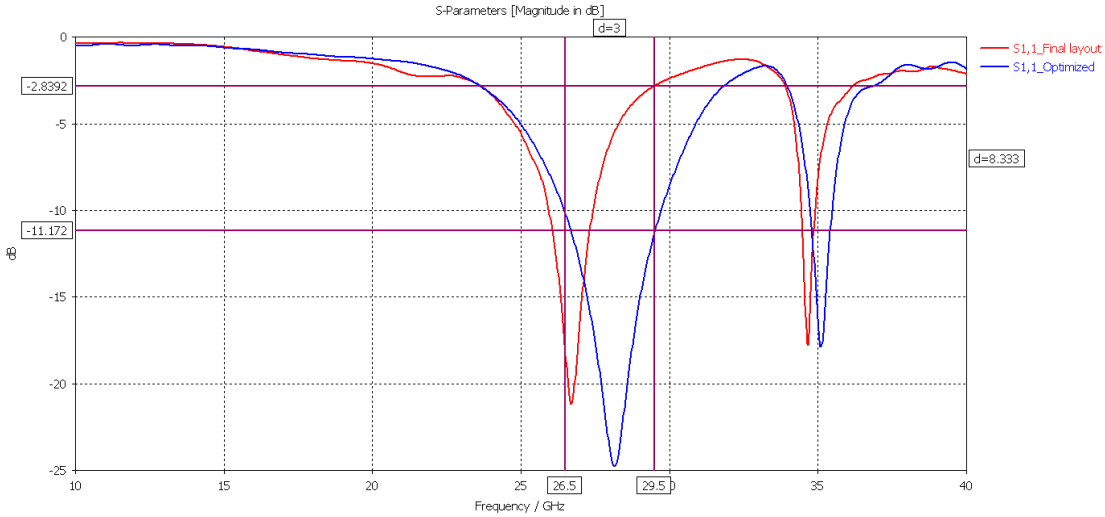

Fig. 26. S_{11} simulation results for GCPW-via-antenna structure – optimized vs. final layout.

By inspecting the layouts and comparing them, there were two reasons affecting the results. The first one is the via diameter, which was set to 0.25mm in the simulations and optimization, and turned out to be 0.22mm at the final layout. The used vias are plugged, meaning that the via is filled with epoxy after metallizing the cylinder. In the converted file, the via diameter is a little bit smaller than original one, because the drilling slightly increases the hole diameter.

The second reason for performance differences is the motherboard stack-up. The hand-made motherboard turned out to be 30 µm thicker compared to one that the layout designer created. The actual thickness difference was found from prepreg layers, which were 6 µm thinner than in the stack-up and there are five of them in motherboard. The reason for the 6 µm decrease in thickness comes from PWB manufacturing. The prepreg layer is used to bond core layers together, and in the final heated pressing, the prepreg reforms slightly decreasing its thickness. This reforming assures that the layers stick together properly. [39]

To overcome the antenna matching problem with a 30 µm thinner stack-up, the antenna patch dimensions had to be tuned to achieve the same S_{11} matching as in the optimization chapter. The parasitic patch antenna had to be widened from its sides by 0.2 mm per side and the height was decreased from top by -0.1 mm. The patch itself widened 0.2 mm from both sides and the height increased 0.15 mm from top. With these changes, the antenna performs as close as possible to achieve performance comparable to the one seen in Fig. 24. The modified antenna has S_{11} matching of -10.18 dB and -9.02 dB on lower and higher frequency boundaries, respectively. Final fixed antenna performance is compared to optimized one, seen in Fig. 27. The performance of fixed GCPW-via-antenna structure is -2.26 dB worse from the higher frequency boundary, while it stays the same at the lower frequency boundary. The on-band performance is about 5 dB worse compared to the optimized result. The 35 GHz unwanted resonance spike is now deeper but with a narrower bandwidth.

For GCPW-via-GCPW, the parameters were re-swept to achieve better performance with a 30 µm thinner stack-up, but the changes didn't improve the performance. Fig. 28 illustrates the GCPW-via-GCPW performance of the final layout with fixings against optimized results. The performance in the desired frequency band has degraded about 3-4 dB from the optimized value; however, it is still below -15 dB which is good enough.

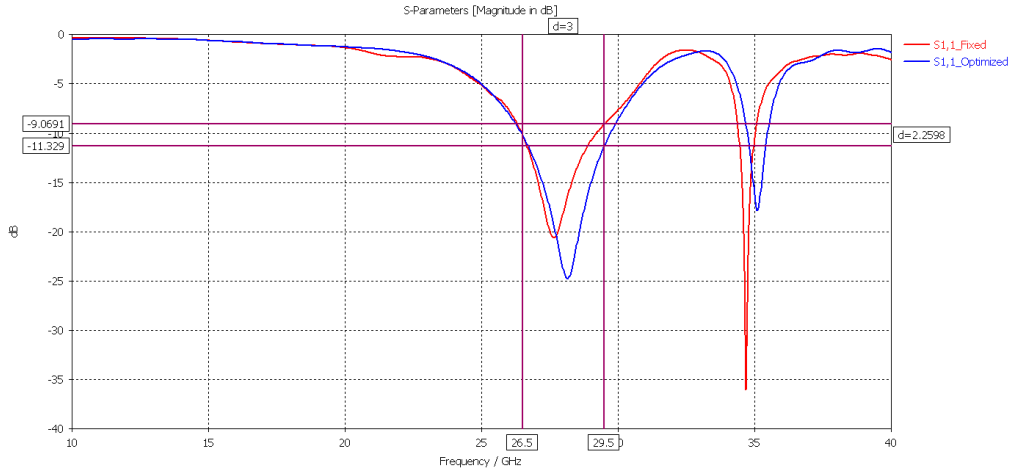

Fig. 27. S_{11} of GCPW-via-antenna fixed vs. previously optimized performance.

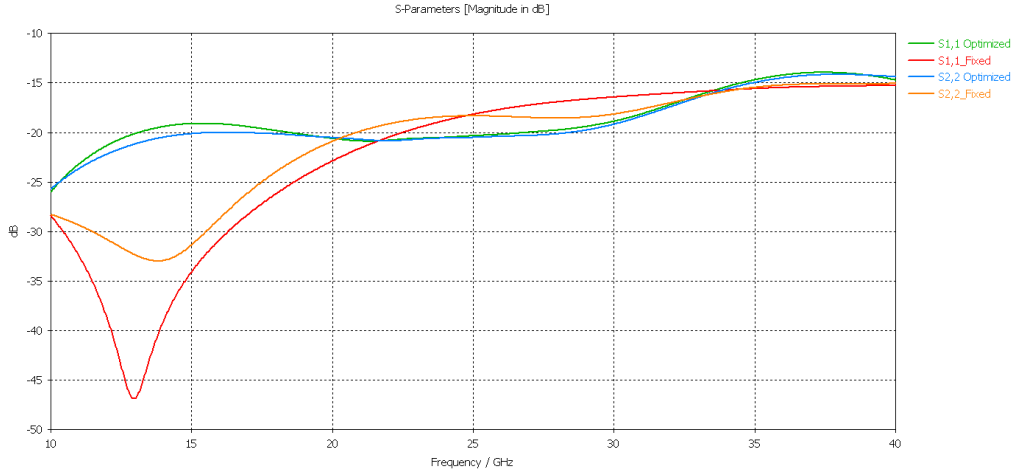

Fig. 28. S_{11} and S_{22} of GCPW-via-GCPW fixed vs. previously optimized performance.

5 PROTOTYPE, MANUFACTURING AND MEASUREMENTS

After finishing the prototype design part, the PWBs were ordered from the PWB manufacturer. The prototype PWBs go through the Nokia Factory, and the creation process is described in its own sub-chapter, Prototype. In the second sub-chapter, after the prototype creation, the prototype system is measured, and the measurement results are compared to simulated ones. Two PWBs go to failure analysis for further investigation of soldering success, which is described in the third sub-chapter. In that sub-chapter, the relation between failure analysis results and measurements is shown and further analysis is made.

5.1 Prototype

The prototype creation starts with PWBs that were ordered from the PWB manufacturer. From these PWBs, six prototypes will be built and the first thing to do with prototype PWBs was to measure the thickness of antenna modules and motherboard. The thickness of the PWBs was measured by Mitutoyo Sheet Metal Micrometer 389 that has 0.001 mm accuracy [40]. Later after the soldering process, it is easier to calculate the overall soldering height, when the thicknesses for antenna modules and motherboard are known. The thicknesses for both PWBs is shown in Table 2 below. Averagely, the antenna module thickness differs from the reference by 0.013 mm, while the motherboard thickness differs from the reference by 0.038 mm. The difference is much greater in motherboard and is more than the changed difference in thickness in Section 4.4 and it may cause antenna S_{11} malfunctioning.

Table 2. Measured thickness of the antenna modules and motherboard separately

Product	Thickness [mm] (5-point average)	Reference [mm]	Difference [mm]
AM1	1.339	1.326	0.013
AM2	1.343	1.326	0.017
AM3	1.339	1.326	0.013
AM4	1.335	1.326	0.009
AM5	1.337	1.326	0.011
AM6	1.341	1.326	0.015
MB1	2.198	2.158	0.04
MB2	2.185	2.158	0.027
MB3	2.204	2.158	0.046
MB4	2.196	2.158	0.038
MB5	2.196	2.158	0.038
MB6	2.199	2.158	0.041

To achieve the required 120 µm soldering height between PWBs, with the LGA method, the solder bumping is needed. As mentioned in Section 3.1.1, the overall solder thickness is roughly halved from stencil thickness. There might, however, be a problem with solder bumping, because the behavior of combining two solders, bumped and wet is not known. The assumption

is that the soldering height becomes smaller due mixing and reforming. To overcome this problem, it was decided that we need the following stencils: 80 µm to motherboard bottom side for termination resistors, 150 µm to antenna module bottom side for solder bumping and 130 µm, 150 µm and 180 µm to motherboard top side for antenna module soldering. By changing the stencil on motherboard, it should be possible to tune the soldering height to the wanted one.

The solder bumping was easier to do when the antenna modules were in the PWB panel instead of doing it for de-panelled ones due to the small size of de-panelled antenna modules. For that reason, the antenna modules were ordered without de-panelling, and the de-panelling was done at Nokia Factory after the solder bumping, by using a milling machine. For the antenna modules milling process, custom-made jig with an assembly pallet was designed, by a mechanical engineer, to ease the milling process and prevent the movement of antenna modules. After the milling process, the antenna modules are already in a pallet for the assembly machine. This method eliminates the possibilities of antenna modules being set facing down, because the antenna modules don't need to be touched by a human during the process. The de-panelled antenna module can be seen in Fig. 29. The left side of Fig. 29. represents the top side of the antenna module, while the right-hand side represents the bottom side with solder bumps visible.

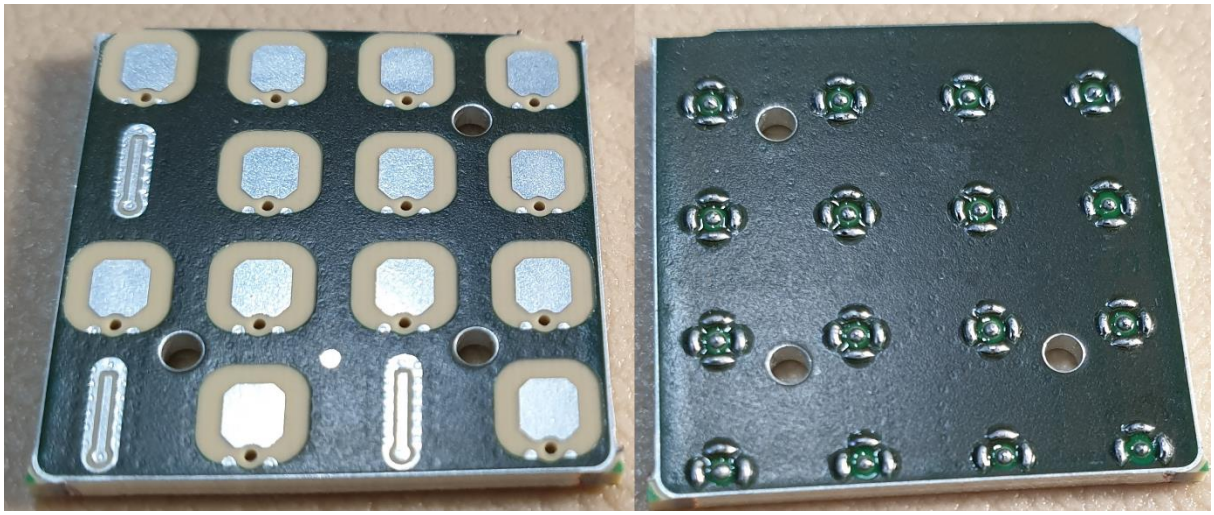

Fig. 29. De-panelled antenna module.

From Fig. 29, one can see that the milling process is not optimal. The milling takes a little bit too much from upper corners, while it leaves small tabs on lower corners. This may come from micro-movements inside the milling jig. Overall, the antenna module still passes the dimension specification to be assembled.

The next step was to apply paste on motherboard with a 150 µm stencil and assemble the components, i.e. antenna modules, and take it through the reflow oven. When the PWBs have cooled down, the overall thickness of the system is measured, and the soldering height can be calculated by

$$H_S = T_P - T_{MB} - T_{AM}, \tag{9}$$

where H_S represents the soldering height, T_P means the thickness of the whole prototype, and T_{MB} and T_{AM} represent the thickness of motherboard and antenna module, respectively. The goal for the soldering height, H_S, is set to 120 µm and after manufacturing the first prototype, the average soldering height is 212 µm (16-point average from the antenna module). An image of prototype can be seen in Fig. 30, below. The result indicates that the soldering height did not half as expected, it only decreased about 30% from stencil thicknesses. One possible reason may be that the reflow oven temperature is not enough to reflow the solder from the antenna module fast enough.

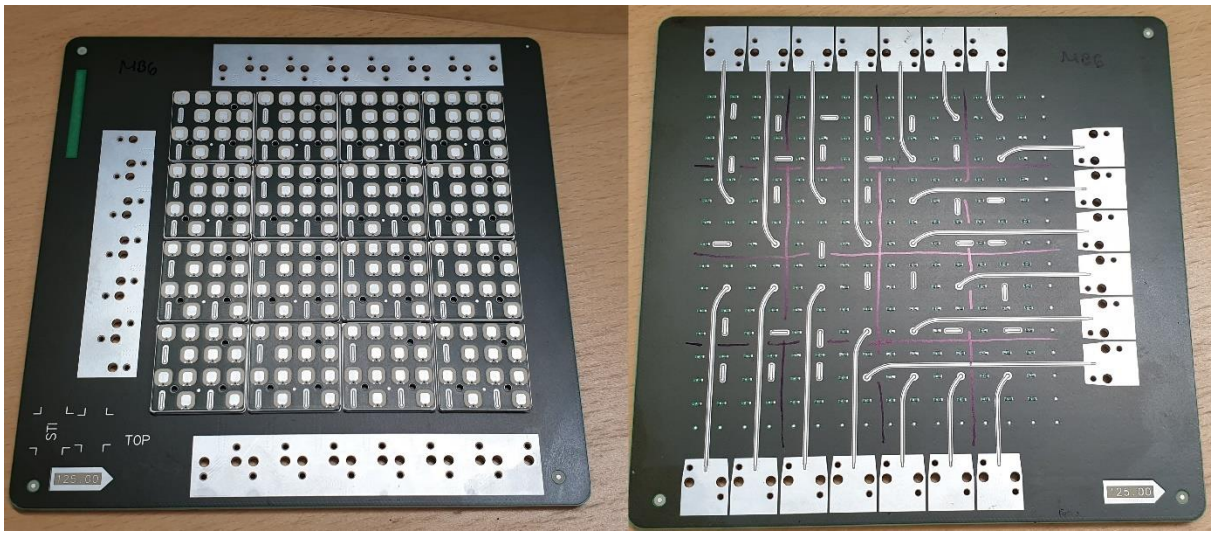

Fig. 30. Prototype from top side and bottom side.

According to the result, the used stencil combination for solder bumping, 150 µm + 150 µm, was way too much and another test round was needed. The next round (prototype 2) was done with only a 180 µm stencil on motherboard and without solder bumping on the antenna module. This should lead to 90 µm soldering height. The average result for soldering height was 89 µm, which can be considered as 90 µm, which was half from the stencil thickness as supposed. From these results, it was possible to summarize that we either need about a 240 µm stencil on motherboard alone or about a 90 µm stencil on both, motherboard and the antenna module with solder bumping. However, the stencil manufacturer has stencils with a step of 30 µm and the closest one to 240 µm is 250 µm, which is close enough. The combination of 90 µm + 90 µm stencils should lead to about 120 µm overall thickness according to earlier results, with 30% degradation from stencil thicknesses. These stencils were ordered.

The next prototypes were done by using solder bumping with a 90 µm + 90 µm (prototype 3) and 250 µm (prototype 4) stencil. The soldering height for prototype 3 turned out to be 137 µm, while prototype 4 gave 130 µm with a 250 µm stencil without solder bumping. According to these results, the fourth prototype is closest to 120 µm soldering height and the last two prototypes (prototype 5 and 6) were assembled using a 250 µm stencil. The solder heights for prototypes five and six was measured to be 125 µm and 122 µm, respectively. Table 3 summarizes the overall solder heights for prototypes. According to results in Table 3, the functioning prototypes are prototypes because they are close enough compared to the target.

Table 3. Solder heights for prototypes

Prototype	Solder height [µm]	Used stencil [µm]
1	210	150+150
2	90	180
3	137	90+90
4	130	250
5	125	250
6	122	250

After all the prototypes were finished, it was possible to inspect the assembly success of the antenna modules. To help this process, there are drawn lines on top of motherboard where to install the antenna modules, and the lines also help in visual inspection after assembly process. The figure of a few antenna modules and drawn lines under them can be seen in Fig. 31. By looking the figure, one can see that the antenna modules are following the drawn lines, so they are set properly, they are not misaligned and the gap between the antenna modules seems to be constant. By inspecting the prototypes from the sides, the antenna modules seem to be set properly with no tilting or bending, except on one antenna module on the first prototype with one antenna module tilted from the lowest row. The prototypes were also inspected with x-ray and according to x-ray figures, the soldering looks good, but in some points, the soldering is asymmetric. The asymmetric solder, seen in Fig. 32 top left corner, should not affect measurement results because the asymmetric shape is in the ground soldering instead of in a signal soldering. However, there was some variation in a signal soldering diameter that may affect measurement results and this variation is also illustrated in Fig. 32.

The plugged signal vias makes it difficult to see whether there is a void or not at the signal soldering spot. However, in Fig. 32, there can be seen a huge void at signal soldering, that is marked with a blue box. In that signal trace, one can see two white rings with a different diameter, from which the smaller one is signal via and the larger one is the void itself. Also, in that case, the signal solder seems to have an increased diameter, which is a reason of having a huge void inside solder.

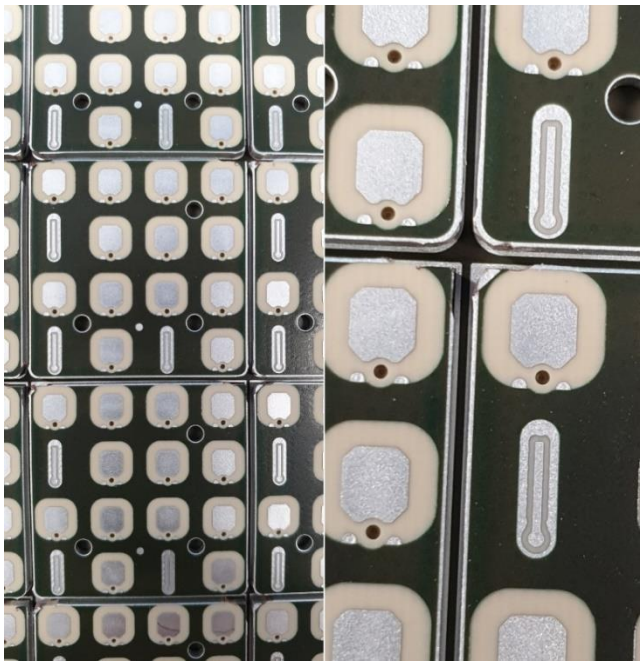

Fig. 31. The visual inspection of antenna modules on motherboard.

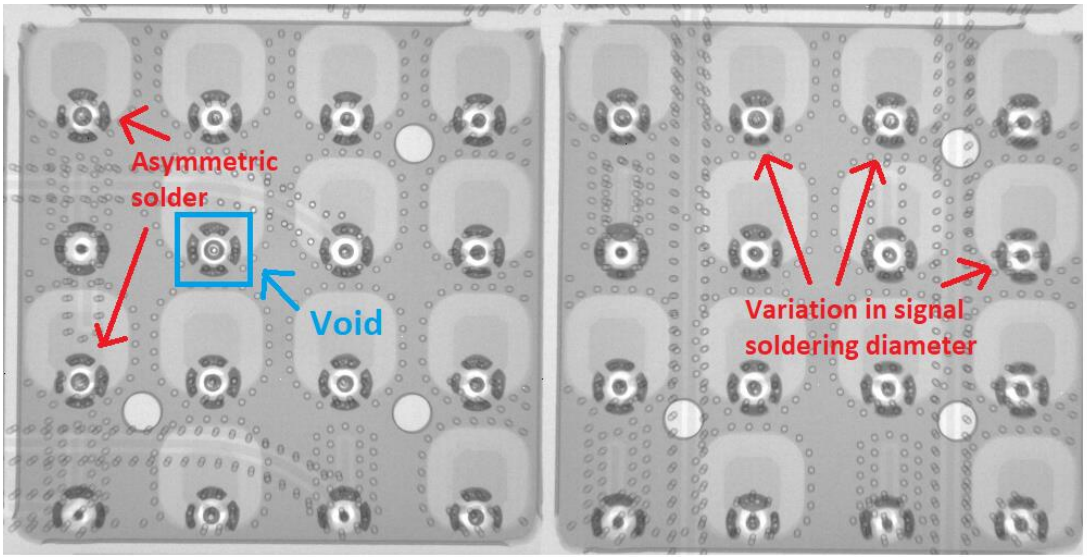

Fig. 32. X-ray inspection for a prototype.

In summary, the prototype creation process was successful when considering the visual inspection and measurement of soldering height. The prototype six seems to be the best prototype due to its soldering height being the closest to the targeted. The RF-measurements for these prototypes are carried out in the next chapter.

5.2 Measurements and results

The measurements were done in a probe-station that is equipped with a microscope on top of PWB and under the PWB. The measurements were done with Keysight PNA-X Network Analyzer which can measure up to 50 GHz. On the motherboard side, there is a possibility to

use an additional RF-connector that can be installed to the motherboard with screws. The used RF-connector is Rosenberger 08K80A-40ML5, functioning from DC-voltage to 70 GHz, with return loss more than -19 dB from 26.5 GHz to 40 GHz [30].

The probe station calibration was already made ready for the measurements (with WinCal XE 4.7, 2-port LRRM-method (Line-Reflect-Reflect-Match) by using Z-Probe GSG-450 probe heads) and the calibration was verified with thru measurement that indicated -35 dB S_{11} accuracy. The first measurements were done to GCPW-via-antenna structure, because it requires only one probe and it was able to carry out measurements from upside, when turning the antenna module side facing down. After GCPW-via-antenna measurements, another microscope and probe were set and the GCPW-via-GCPW measurements were done. All the prototypes were measured even though only prototypes 4-6 are closest to the targeted soldering height. The measurement setup for GCPW-via-antenna (left) and GCPW-via-GCPW (right) measurement can be seen in Fig. 33. To ease the measurement process, the antenna modules were named, and antenna module lines were drawn underside of motherboard. The naming starts from the top left corner with the name AM1 (antenna module), when looking from the top side of the prototype and goes from left to right row by row, meaning that the last antenna module on the lower right corner is named as AM16.

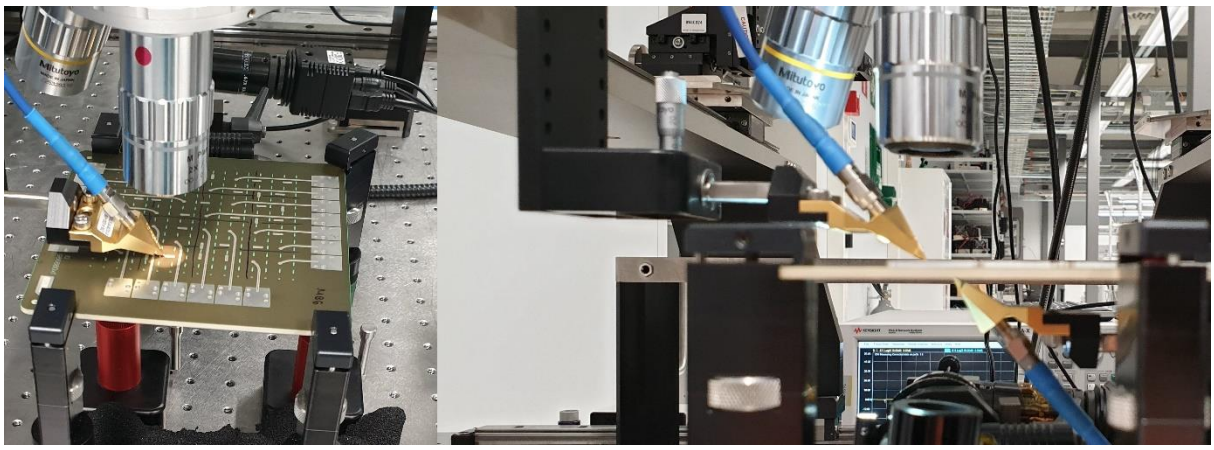

Fig. 33. Measurement setup for GCPW-via-antenna and GCPW-via-GCPW measurements.

When measuring the GCPW-via-antenna structure, the measured antennas from antenna modules were the following: AM2, AM4, AM9, AM10, AM15 and AM16 and they were chosen because the GCPW-line is pointing upwards or downwards, when looking from the bottom of the prototype. Furthermore, the lines that are pointing left or right are located too close to termination resistors and those lines cannot be measured because the probe hits the resistors before hitting the GCPW-line.

Fig. 34, illustrates the average result from measured S_{11} performance against simulated one with a 120 µm solder height, with blue and red colors, respectively. The used GCPW-via-antenna structure was from prototype 3 AM15. As mentioned in Section 4.2, the goal for GCPW-via-antenna S_{11} was set to -10 dB. According to the measurement result in Fig. 34, the matching on lower and upper frequency boundaries are -8.62 dB and -11.42 dB, respectively. The results indicate that the resonance dip is where it should be and by comparing the shape of

measured result against the simulated one, the prototype has a wider band after 29 GHz, leading to better performance on a higher frequency boundary. The envelopes of measured result and simulated one are somehow similar, but the measured one is shifted about 1-1.5 GHz toward higher frequencies, when comparing the maxima and minima. The frequency shifting may come from changes in PWB stack-up, asymmetric soldering shape or from a different solder height, as discussed in Chapter 4. Furthermore, the accurate information about PWB stack-up can be achieved by doing failure analysis (more in the next sub-chapter). Additionally, the GCPW-via-antenna structure has many alternative resonance frequencies after 30 GHz and those must be eliminated if the antenna is meant to be used in a product.

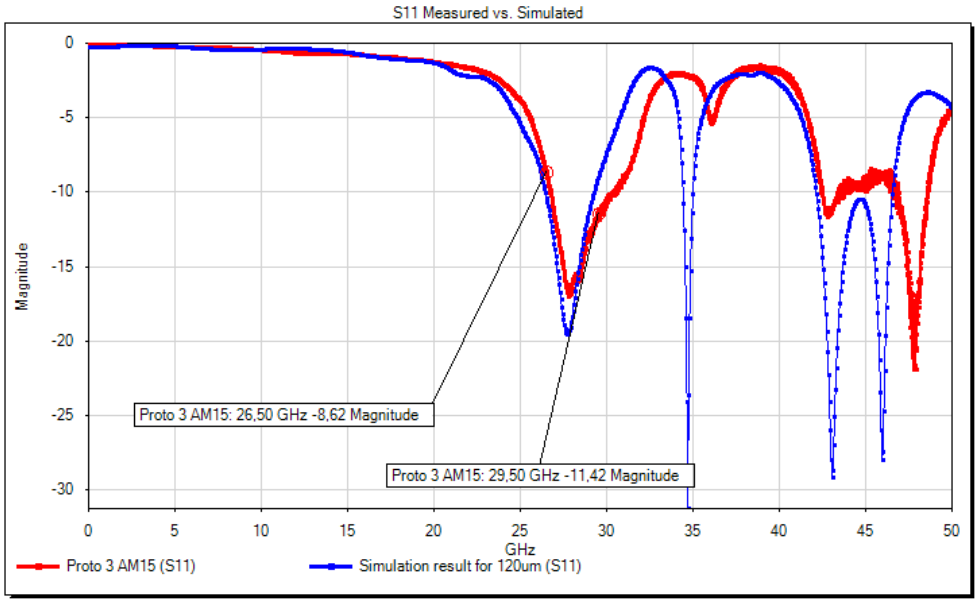

Fig. 34. S_{11}-measurement results for GCPW-via-antenna.

The GCPW-via-GCPW structures were added to the prototype to measure matching and losses from prototypes. Fig. 35 shows the average result from S_{11} and S_{22} measurements against simulation data. The average measurement result is taken from prototype 5 AM4 and the simulation data is with a 120 µm solder height. The measured result is better on the desired frequency band until the frequency of 28.6 GHz, compared to simulation. The matching values on lower and upper frequency boundaries are -27.11 dB and -16.11 dB, respectively.

The S_{12} and S_{21} measurement results of GCPW-via-GCPW structure are shown in Fig. 36. According to that figure, the maximum loss at the end of frequency band is -0.85 dB, which is better than that obtained with the given -1 dB goal. The measured losses differ -0.21 dB (at 29.5 GHz) from simulation results. With the given -1 dB goal, that structure is functional up to 30.5 GHz.

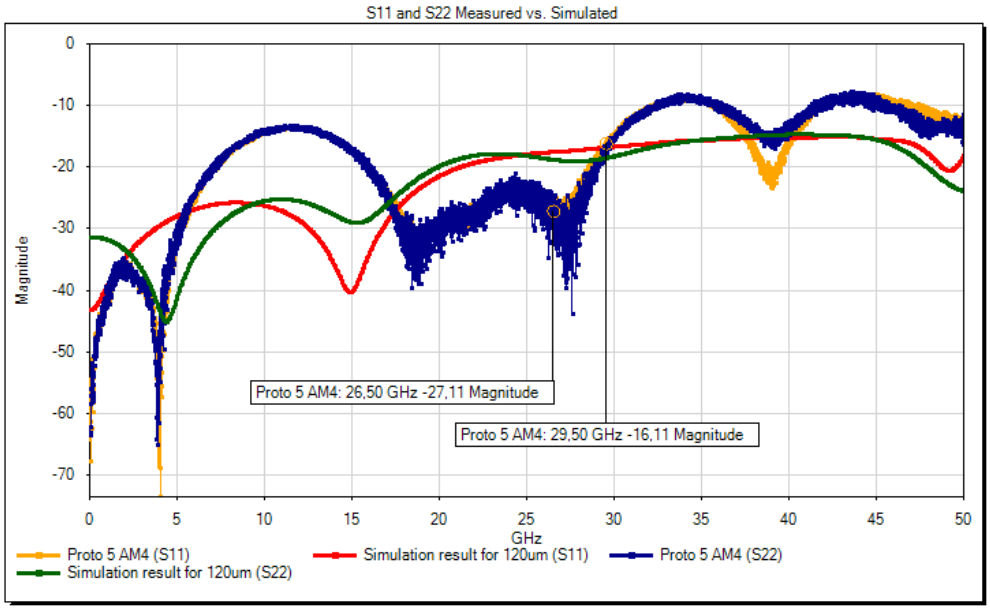

Fig. 35. S_{11} and S_{22} measurement results for GCPW-via-GCPW structure.

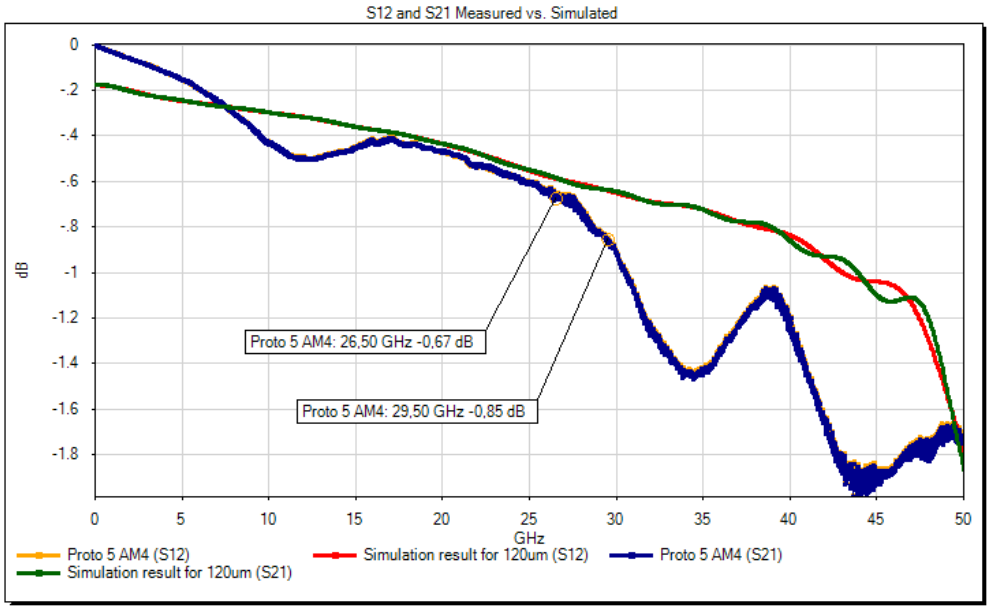

Fig. 36. S_{12} and S_{21} measurement results for GCPW-via-GCPW structure.

After probe measurements, there was a plan to do the measurements by using RF-connectors. Unfortunately, there had been a mistake in RF-port layout design and because of that mistake, the RF-connector pin does not connect with GCPW-line. There was a possibility to widen the holes for RF-connector to get the connection between pin and GCPW-line, but the measurement results were enough, and it was not done.

Overall, both GCPW-via-antenna and GCPW-via-GCPW -structures seem to be functional, but they differ from the simulation results. As mentioned before, the shown simulation results are nominal values and the results vary around the nominal value, creating a difference between

measurement and simulation, to see the variation, see Attachment 1. Further analysis of factors affecting differences in results, are discussed after failure analysis.

5.3 Failure analysis

After the RF-measurements, two prototypes were taken to failure analysis. By doing cross-sectional failure analysis, the success of soldering can be really seen, and the overall soldering height can be measured, also the dimensions of a few different antennas were measured. In this approach, the prototype PWB is cut half from the desired spot, and the cut edges are refined for analysis. If the PWB is cut close to signal via, the soldering height can be inspected after refining. Additionally, by looking at the antenna module, one can see whether the module is bending, tilted and soldered properly. In this section, the dimensions of antennas were inspected, and failure analysis was done to two prototypes.

Before cutting any prototypes, the dimensions of antennas in antenna modules were measured with a microscope. This way, the average difference between antenna modules can be found and the result may help understanding the variation in measurement results. However, it was only possible to measure the parasitic patch because it is visible. The measurements indicated that the antenna patches are averagely 25 µm narrower and 20 µm shorter compared to designed measures, while the width varies from -10 µm to -43 µm and length from +1 µm to -48 µm.

The prototypes for failure analysis were chosen to be prototypes 3 and 4 and the reasons for choosing these prototypes are the following: prototype 3 is the only functioning prototype with solder bumping and it has relatively stable measurement results and prototype 4 seems to have many asymmetric soldering and unstable measurement results. The chosen antenna modules from these prototypes were antenna modules 2 and 4 from each prototype, making a total of four pieces to inspect. The chosen interconnection to inspect is the second row from the antenna module and from that row, the columns 1-3, this is illustrated with blue box and red line in Fig. 37 below, where the red line illustrates the exact spot. The GCPW-via-GCPW and GCPW-via-antenna measurement were carried out for both prototypes and antenna modules from this spot making it easy to compare the failure analysis results to measurement results. However, the interconnection in the middle of the box was not measured, because it is a dummy antenna.

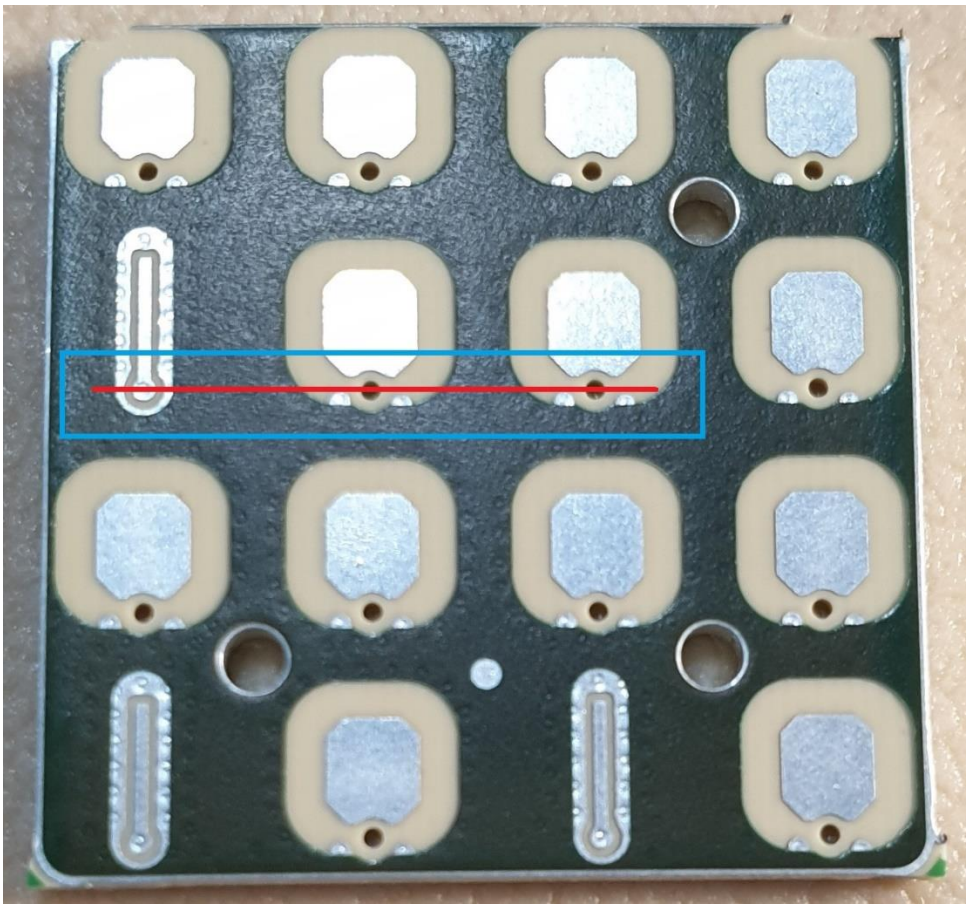

Fig. 37. Interconnections under failure analysis inspection.

The cross-sectional failure analysis started by cutting the PWBs close to the interconnection under inspection. The edges were sanded, and the models were molded in transparent epoxy. After the epoxy was dry, the models were again sanded until the wanted spot was reached, and then the models were refined and polished for better inspection visibility and were ready for visual inspection with a microscope, the model can be seen in Fig. 38 below. Additionally, the microscope can take an image of view and has a possibility to measure different distances from the microscope image, which helps the analysis of the results.

When visually inspecting the prototypes, the antenna modules seem to be accurately assembled. However, there were small misalignments that were found from the cross-sectional view, but no bending was found from the antenna modules. For example, one way to illustrate the misalignment is looking at the signal via, the via on the antenna module was totally visible, while the via on the motherboard side was only partly visible.

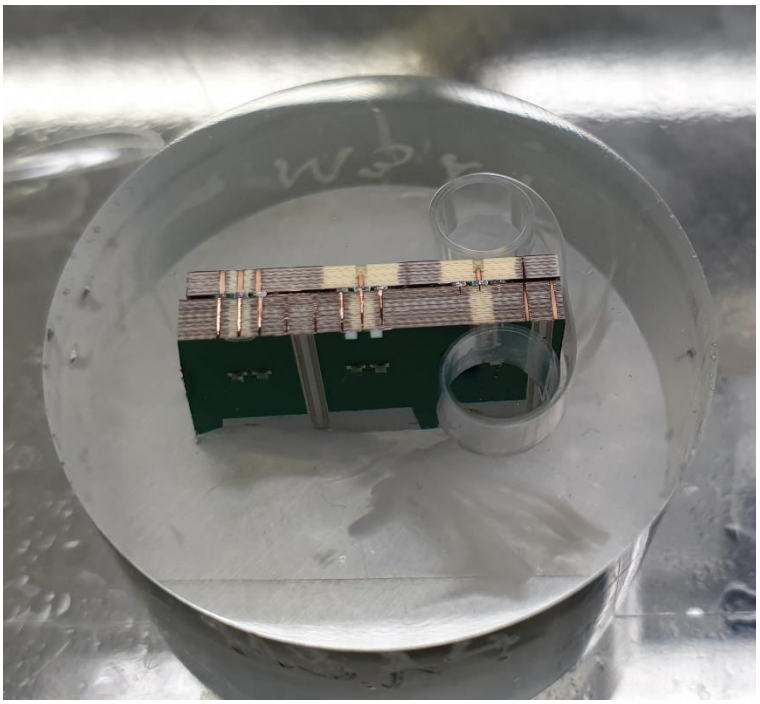

Fig. 38. Molded model that is refined and polished.

By doing failure analysis inspection for the molded model, seen in Fig. 38, further information from the following properties was obtained: stub height after back drill, solder dimensions and shape, appearance of voids in solder and PWB stack-up, including pad sizes, etc. Variations in these listed properties have effects on measurement results because they influenced results in simulation and optimization work. To illustrate the following properties, Figs. 39-41 are presented, and they include cross-sectional images, x-ray images and S_{11}-measurement results for AM2 or AM4 between prototypes 3 and 4. From the figures, Fig. 39 presents the GCPW-via-antenna comparison for AM2, while Fig. 40 includes GCPW-via-antenna comparison in AM4, and finally, Fig. 41 has the comparison for AM4 GCPW-via-GCPW structures, between the prototypes.

In Fig. 39, the S_{11}-matchings differ from each other and the idea of the image is to illustrate a reason for these differences using cross-sectional image and x-ray image. In this figure, the prototype 3 represents a nominal situation, while prototype 4 is compared to it. When comparing the solder joints between prototypes, a few notes can be made. Firstly, the solder in prototype 4 seems to widen about 100 µm over the solder pad and it also widens over the solder mask (seen as light green next to the black solder pad). This widening leads to variation in signal solder that can be seen in the x-ray image, as noticed in Section 5.1 in Fig. 32. Another finding is that there are voids, but more importantly, the voids are larger in prototype 4. The third finding is that the shape of the ground soldering differs on left and right, making it asymmetric. The results clearly indicate that these findings affect performance by decreasing the matching in prototype 4.

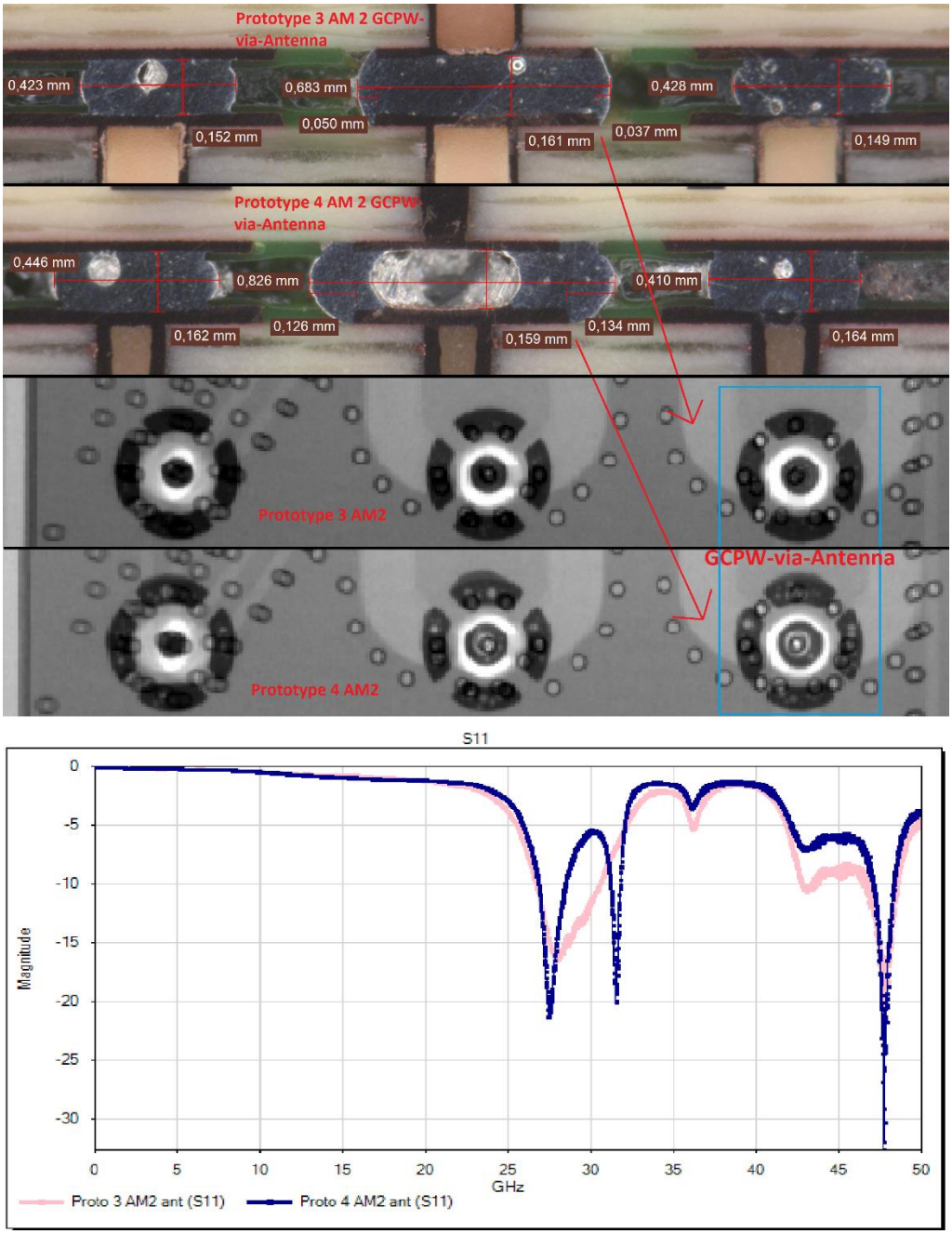

Fig. 39. The cross-sectional images, x-ray images and measurement results for AM2 GCPW-via-antenna, between prototypes 3 and 4.

In the case of Fig. 40, S_{11}-parameters vary slightly from each other. The solders seem good, except the left ground at prototype 4, that has widened over the solder mask and has a huge void inside. The solder height of prototype 4 seems to be 18 µm thinner, averagely, compared to prototype 3 and the signal solders have widened the same amount in both prototypes. The x-

ray image shows that the prototype 4 has asymmetric soldering and an asymmetric solder with a different solder height which seems to give slightly decreased performance to that prototype.

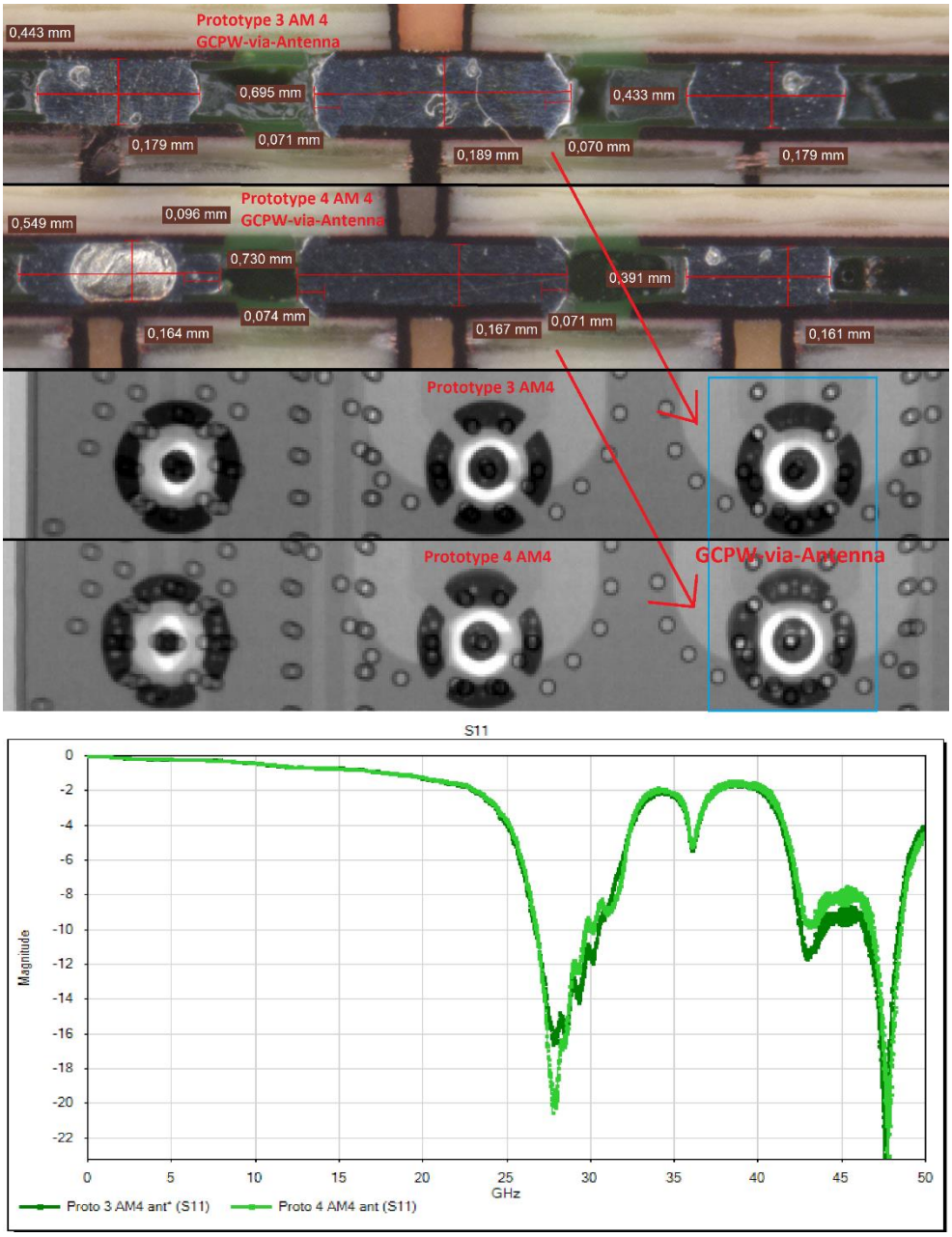

Fig. 40. The cross-sectional images, x-ray images and measurement results for AM4 GCPW-via-antenna, between prototypes 3 and 4.

Finally, when inspecting Fig. 41 S_{11}-parameters, there is only a small difference between results. The ground solders seem good, except prototype 4 left ground, which has widened over the solder mask and has a huge void inside. However, the prototype 4 signal solder differs from others, so far. The solder is a lot narrower than solder pads and the narrowness can also be seen in the x-ray image. In the optimization part, it was noticed that the smaller the diameter of signal pad is, the better the matching. According to these results, prototype 4 matching is better, and the difference most probably comes from the narrow signal solder, because asymmetric solders or other findings were not found.

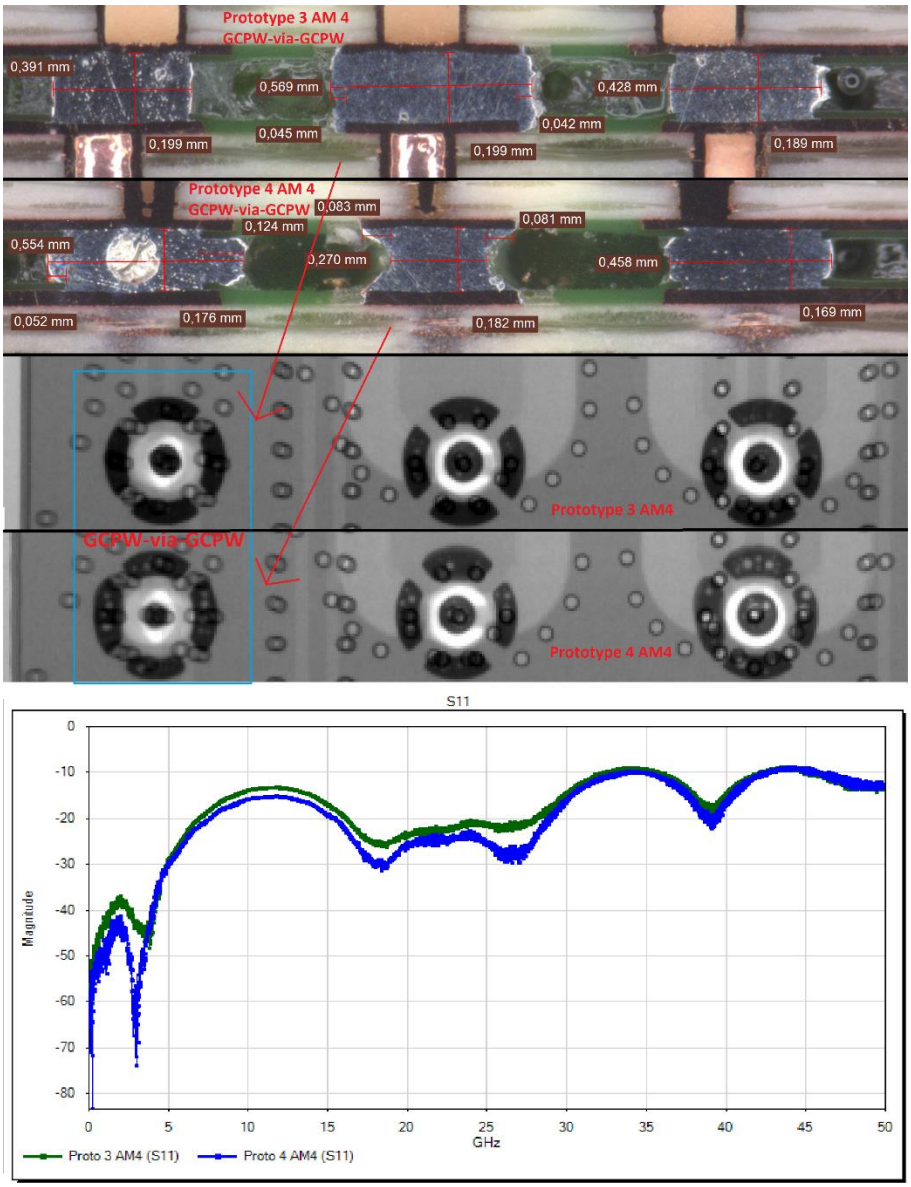

Fig. 41. The cross-sectional images, x-ray images and measurement results for AM2 GCPW-via-GCPW, between prototypes 3 and 4.

To summarize the findings from Figs. 39-41 and from failure analysis, prototype 3 seems to have less and smaller voids, compared to prototype 4 and prototype 4 has widened solders that also leads to an asymmetric solder, and according to results, these both decrease the matching. In addition, the results indicate that the small misalignments do not have effects on matching. Prototype 3 was created by using solder bumping with thinner stencils, while prototype 4 had only one 250 µm thick stencil. According to failure analysis results, the solder bumping leads to less and smaller voids. The solder bumped antenna module has one already melted solder where flux has faded and when it is assembled on top of a wet solder, there are, logically, more space for flux to fade from the wet solder. Furthermore, when using a 250 µm stencil between PWBs, there are less space for flux gases to fade, that seems to lead to huge voids. Additionally, these huge voids seem to widen the solder, because that gas stays inside the solder making the solder paste resettle. However, it was tested with simulation whether the huge void influences

matching or not, and the results indicate that it does not matter at all if the void is in the middle and the size of the void did not have any effect at all. The reason behind this can be found from the skin effect, which is less than one micron at mm-wave frequency making the currents flow close to the outer edge of conductor [41].

In addition to these findings from Figs. 39-41, PWB stack-ups and height of back drilled stub was measured. The back drilled stub height average stub height became 120 µm, while it had a minimum of 101 µm and a maximum of 136 µm. The stub is problematic due its discontinuity that leads to unwanted reflections affecting matching properties, as mentioned in Section 4.1.3. According to these results, the stub is averagely 20 µm higher than the one used in simulations. The 20 µm increase in stub height decreases the antenna performance about 0.13 dB on the lower frequency boundary and 0.1 dB on the higher frequency boundary. The effect of 136 µm stub was also tested and the degradation (compared to 100 µm stub) was about 0.24 dB and 0.19 dB, respectively. Overall, the differences in stub height only fine-tune the antenna matching.

The PWB stack-ups were calculated by using the measuring option in microscope software. Both prototype 3 and 4 were measured and the results are presented in Table 4 below. According to the table, the prototypes had a smaller or equal stack-up compared to the one that was used in simulations. However, in the case of the antenna module, the first given model from the layout designer had thickness of top and bottom metallization layers of 0.045 mm instead of 0.05 mm, which leads to an 0.01 mm difference between design and simulation and the same change in metallization thickness was used in motherboard. The motherboard had thicker stack-ups compared to designed or simulated ones and the reason for that may be the variation in thick layers. However, in simulations, the motherboard was insensitive to these thickness changes.

Table 4. Measured PWB stack-up thicknesses against designed and simulated one

Measured item	Prototype3 [mm]	Prototype4 [mm]	Designed [mm]	Used in simulation [mm]
AM Stack-up	1.323	1.346	1.356	1.346
MB Stack-up	2.204	2.207	2.158	2.12

From the functionality point of view, the measured prototypes seem to function properly, also both GCPW-structures function properly. The matching was optimized in Chapter 4, and the measurement results follow the optimization results with small variation. However, the simulation results differ from the measurement results and the reasons were investigated. The deeper analysis of variation in results includes aspects from prototype design, manufacturing processes and measurement setup, as well as the measurement method itself. The obtained information from this chapter teaches what should be done differently to achieve better functioning of the prototype or correlation between simulation and measurement results.

The GCPW-via-antenna and GCPW-via-GCPW performance is close to what it should be with a few exceptions. These exceptions include alternative resonances on higher frequencies (antenna), wider bandwidth (antenna), frequency shifting and overall variation between measurement results that can be seen when putting all the results in the same figure. The

possible reasons explaining the differences can be categorized as follows: design, simulation, x-ray, measurements and failure analysis. These reasons are explained separately below.

The design part was a long process with many different choices. One of the choices was to put the de-paneling connecting tabs to the corners. After milling process, it was noticed that the cutter removes too much from the upper corners of the antenna module. The patch antenna has an opening around the upper corners and after the opening, there are ground layers that are grounded with vias fences. The milling process removes too much PWB material from corners reducing the grounding by removing ground vias which may lead to signal leakage [16]. Additionally, other thing related to antenna module design is the hold-hole location. The hold-hole on the right upper corner of antenna module should be on the left corner, instead of next to the measured antenna. The hole is coppered from its inner edge, so the antenna surrounding may seem different to that direction. These can be considered as major reasons in design part, that may lead to decreased matching.

There was also one layout mistake in the motherboard PWB related to RF-connector that may cause the difference between simulation and measurement result. The RF-connector pin does not connect to the GCPW-line. As seen in Fig. 30, the GCPW-lines can go from the middle of motherboard to outer edges and when the RF-connector is not connected, the surroundings seem different for the points under measurement. To avoid this, the floating RF-connector routes should be terminated to 50 Ω, as mentioned in Section 4.1.4. However, the termination was not done, and those floating lines may make the differences between measurements and simulations.

The simulation setup and parameters may lead differences between measurement and simulation. For example, the copper surface roughness (chosen value can be set in CST) is one important parameter to consider in mm-wave frequencies. The surface roughness indicates how rough the edge of surface is from its peak-to-peak value [42]. Other thing related to surface roughness is skin depth. Skin depth describes how current is distributed, for example, in a round conductor and the skin depth is less than a micron at mm-wave frequencies [41]. This means that the current is flowing close to edge of surface when operating on higher frequencies [41]. If that surface is rough with a high peak-to-peak value, the flowing current goes up and down all the peaks leading to increased path length and resistance [42]. This may have huge effects on simulation results. However, also the measured dielectric constant and loss tangent might influence differing results.

When the prototypes were manufactured, they were measured at a probe station, which was already calibrated. One way to minimize the changes in measurement results is to always measure from the same spot of the GCPW-line. In measurements, when looking from top of the antenna module (seen, in Fig. 29 left), the used spot was vertically on top of the signal conductor, i.e. where the GCPW-line ends, while it was horizontally centralized to the middle of the GCPW-line ending. The CST simulation software uses the same port location but using a waveguide port. Using this method, the difference between simulation and measurement is minimized.

According to x-ray images, the soldering can be asymmetric, and the signal solder diameter has some variations. The asymmetric soldering and diameter variations may come from soldering paste or stencil. The soldering paste itself is called pseudoplastic, which means that

it moves easily when pushing it and when more pressure is applied, the easier it runs, but when it is left alone, it gets stiff and doesn't lose its shape [17]. This means that the soldering paste should run well, but the problem may come from the fact that the solder paste does not detach from the stencil properly. The stencil is thick, for example, in prototypes 4-6, 250 μm, and the holes are small, especially in sectorized groundings. This means that some of the solder paste might not detach properly, making the soldering asymmetric. The asymmetric soldering itself changes the grounding properties, when comparing to the point with symmetric soldering, leading to differences in measurement results.

The final information about the success of the prototype was achieved from failure analysis. According to failure analysis, the antenna modules are properly assembled, and no bending was found. In addition, small misalignments were found but they did not have any effects on matching. The major reason for varying measurement results was found out to be the shape of the solder. Using the solder bumping, less voids appear, leading to well-shaped soldering between PWBs. When the solder bumping was not used, the flux gases have less space to fade away, leading to huge voids inside the soldering, which again leads to a widened solder joint. The widened solder joint with an increased solder height leads to the maximum of 0.5 GHz frequency shifting on the frequency band and about 50 MHz frequency shifting on higher frequencies. However, this 0.1 GHz on higher frequencies is not enough to explain the frequency shifting problem between simulation and measurement results but might be one reason behind it, nevertheless.

The appearance of voids also effects on ground soldering, making the ground soldering asymmetric, which in its turn leads to decreased matching properties. Additionally, a huge void inside a signal solder leads to a widened frequency band of antenna, as seen in Fig. 39. Above, it was discussed if the solder paste does not detach properly, but this information makes the solder detaching issue invalid.

The findings above do not clearly point the reason behind frequency shifting between simulations and measurements. However, these findings may be the reason, but further investigation was done in CST. First, the effect of solder mask between soldering was tested. According to the PWB manufacturer, the solder mask has ε_r about 3.5, which means that it should be considered, especially because the solder itself sometimes widens between two solder masks. In addition to the solder mask test, it was tested whether the distance between signal solder and ground solders has impact on frequency shifting. The frequency shifting at higher frequencies was 0.1 GHz at maximum and it was found, when both ground solders were moved 100 μm closer to the signal solder. However, this also worsens the antenna matching properties on desired frequency band.

Overall, many reasons behind differences between results were found and many of them can be minimized or fixed. The main reason leading to bad soldering seem to be void that comes, when using thick stencils instead of solder bumping. This, together with other findings, can explain most of the differences well enough. However, the reason for frequency shifting at higher frequencies was not totally found but all findings above may have effects on that shifting.

6 DISCUSSION

The aim of this thesis was to provide a functional and optimized interconnection method with measurement results and limitations of Nokia Factory to Nokia. With the knowledge from this research work, this new method can improve the level of integration in a possible product, while increasing the cost-efficiency simultaneously. The increased cost-efficiency comes from smaller dimensions, thinner PWBs and easy manufacturing process. In the opinion of the author, the goal of this thesis was reached, because the interconnection method was found, optimized and the limitations of Nokia Factory were considered. Additionally, reasons behind different measurement results were also found and analyzed.

Overall, the experiment was successful, it did teach a lot and gave important new knowledge about the possibilities of vertical stacking as a part of a possible product. Naturally, there are always things that went as expected and things that require improvements. To further improve the prototype or a possible product, there are a few recommended changes. Firstly, the antenna should be especially designed for this kind of structure: the one designed in this thesis was for a totally different stack-up and converted to a new stack-up. The radiation properties of the antennas will most probably be different due to changes in patch dimensions, stack-up, and the most importantly, with an added air-cavity between PWBs.

Another thing to consider, to minimize the variation in soldering height, is that the BGA interconnection method should be better, especially PBGA, because it provides a controlled solder height between PWBs. However, if the LGA method must be used, for example, because the BGA installation takes time and needs some investments, the LGA interconnection should be done by utilizing solder bumping. Furthermore, with solder bumping, the gap between sectorized grounding should be increased to provide enough space for flux gases to fade, avoiding appearance of voids. In addition to the interconnection method and antenna, the found problems at Section 5.3 are still valid and must be considered, if there were another prototype round.

To fully understand the different aspects affecting results, the simulations should be re-done as follows: using the layout according to failure analysis, by using different shapes of soldering between signal pads, using different surface roughness for copper, decreasing the dimensions of the antenna according to failure analysis and by considering the distance between signal solder and ground solder.

7 CONCLUSIONS

This research work provides material for creating interconnections between PWBs, when working on mm-wave frequencies. In this thesis, antenna module and motherboard were partly designed and a suitable interconnection method, for connecting antenna modules and motherboard, was chosen. An antenna array of 256 antennas was created by connecting sixteen antenna modules (each with an antenna array of 4x4 antennas) to motherboard. From that antenna array, 48 antennas were replaced with GCPW-lines for measuring purposes (three antennas from each antenna module). The background for this thesis was to reduce the overall price of a possible mm-wave frequency product, while making the system more integrated by applying vertical stacking. The price and dimensions of possible product can be decreased by using the method that was introduced in this thesis.

In this thesis, basic microwave theory or background was provided for gaining better understanding of the design part. The basic theory gives good understanding about antennas, antenna arrays, GCPW-lines, S-parameters and wideband impedance matching. These all were needed in the design part to achieve a fully functioning structure.

The suitable interconnection method between PWBs was chosen between three options: soldering, RF-connector or Molex array connector. The most suitable interconnection method turned out to be soldering, by applying LGA-method. LGA-method was chosen, because the standoff height was critical between PWBs and LGA connection was easy to utilize. However, the BGA method would have been better due to more reliable soldering and higher standoff, but it would require a huge number of working hours or other investments for soldering ball installation.

After choosing the suitable connection method, the optimization process for ready structure, including the antenna modules, motherboard and interconnection, was carried out. The design process started by verifying the non-mm-wave material performance on mm-wave frequencies by doing material tester measurements. According to these results, the material can be used for mm-wave frequencies. The design process continued with design of PWB stack-up, introduction and design of GCPW-via-GCPW- and GCPW-via-antenna structures, design for the antenna modules and motherboard, design of soldering between PWBs, and finally, the optimization for both structures, using parameter sweep and modeFRONTIER optimization software. The optimization results were compared against simulation results that were achieved by simulating using default values. According to simulations, the optimization was successful, and the optimized values were used for the final layout. The functioning of the final layout was verified, and small changes were needed due to material thicknesses and via structures. These changed led to a small degradation in performance, when comparing to the optimized performance. The PWBs were ordered after the verification process.

The first thing with PWBs was to measure the thicknesses of all PWBs for later analysis. The prototypes were created by using different stencils and with- or without solder bumping. The prototypes 3-6 were considered as fully functional and they were measured. Measurement results indicated that there are a lot of variation between measurements and the results also differ from simulations. The reason for measurement results differing from simulations, was found from x-ray and failure analysis. According to x-ray and failure analysis, the solder

bumped prototype has less and smaller voids compared to the prototype that was made by using one stencil. The appearance of huge voids widens the solder itself, leading to decreased matching properties. Furthermore, the widened solder leads to asymmetric ground soldering, which again decreases the matching.

The success of thesis work was discussed in the last chapter, which also included some improvement ideas for possible research work in the future. In summary, the experiment was successful but if there were a next round of prototypes, the recommended interconnection method is PBGA, or if the LGA should be used, solder bumping must be utilized. Another aspect was the antenna itself: the antenna should be designed especially for that purpose, the used antenna was converted from a different stack-up to this one, which most probably weakens its radiation properties.

8 REFERENCES

[1] Nathan Seongheon Jeong, Yu-Chin Ou, Ali Tassoudji, Jeremy Dunworth, Ozge Koymen, Vasanthan Raghavan (2018) A Recent Development of Antenna-in-package for 5G Millimeter-Wave Applications. *IEEE Wireless and Microwave Technology Conference (WAMICON) 19th 2018*

[2] Jing Zhang, Xiaohu Ge, Qiang Li, Mohsen Guizani, Yanxia Zhang (2017) 5G Millimeter-Wave Antenna Array: Design and Challenges. *IEEE Wireless Communications 24(2), 106-112*

[3] Xiaoxiong Gu, Bodhsatwa Sadhu, Duixian Liu, Christian Baks, Alberto Valdes-Garcia (2018) Antenna-in-Package Design and Module Integration for Millimeter-Wave Communication and 5G. *IEEE International Symposium on VLSI Design, Automation and Test (VLSI-DAT) April 2018*

[4] Tristan Ossama El Bouayadi, Laurent Dussopt, Gilles Simon, Y. Lamy (2016) 3D Integration and Packaging of mmWave Circuits and Antennas: Opportunities and Challenges. *Microwave Journal. 59. 22-34*

[5] Xiaoxiong Gu, Duixian Liu, Christian Baks, Ola Tageman, Bodhisatwa Sadhu, Joakim Hallin, Leonard Rexberg, alberto Valdes-Garcia (2017) A Multilayer Organic Package with 64 Dual-Polarized Antennas for 28GHz 5G Communication. *IEEE MMT-S International Microwave Symposium (IMS) June 2017*

[6] Xiaoxiong Gu, Duixian Liu, Christian Baks, Jean-Olivier, Plouchart, Wooram Lee, Alberto Valdes-Garcia (2018) An Enhanced 64 Element Dual-Polarization Antenna Array Package for W-band Communication and Imaging Applications. *IEEE 68th Electronic Components and Technology Conference (ECTC) May 2018*

[7] Balanis, C. A. (2005). Antenna theory: analysis and design. John Wiley & Sons.

[8] Trivedi, R.D., Dwivedi V. (2012) Stacked Microstrip Patch Antenna Gain and Bandwidth Improvement, Effect of patch rotation. *IEEE International Conference on Communication Systems and Network Technologies, May 2012*

[9] Sarin V.P., Nishamol M.S., Tony D., Aanandan C.K., Mohanan P., Vasudevan K. (2011) A Wideband Stacked Offset Microstrip Antenna with Improved Gain and Low Cross Polarization. *IEEE Transactions on Antennas and Propagation 59(4), 1376-1379*

[10] Yang Z., Browning K.C., Warnick K.F. (2016) High-Efficiency Stacked Shorted Annular Patch Antenna Feed fo Ku-Band Satellite Communications. *IEEE Transactions on Antennas and Propagation 64(4), 2568-2572*

[11] Rainee N. Simons (2001) Coplanar Waveguide Circuits, Components, and Systems, John Wiley & Sons, Inc (pp 1, 320)

[12] Razavi, B. (2011). RF Microelectronics, 2nd edition, Prentice Hall U.S

[13] David M. Pozar. (2011) Microwave Engineering, 4th edition, John Wiley & Sons Inc. (pp. 195)

[14] Räisänen A., Lehto A. (2011) Radiotekniikan perusteet, Otatieto (pp. 53-71)

[15] Antenna Theory (read 10.1.2019) Introduction to Smith Charts. URL: http://www.antenna-theory.com/tutorial/smith/chart.php

[16] Kangasvieri T. (2008) Surface-mountable LTCC-SiP module approach for reliable RF and millimeter-wave packaging, University of Oulu, URL: http://jultika.oulu.fi/files/isbn9789514289217.pdf

[17] Strauss. R. (1998) SMT Soldering Handbook. Newnes

[18] Wong P.W., Ying M., Tengh A., Mohtar A., Chia Y.C. (2006) Extra Thin Profile Land Grid Array Package Solder Joint Reliability Assessment. *Electornics Packaging Technology Conference 8th 2006, 307-312*

[19] NXP Semiconductors (2008) Manufacturing with the Land Grid Array Package (read 17.1.2019) URL: https://www.nxp.com/docs/en/package-information/AN2920.pdf

[20] Joshi S., Afraei B., Singh A., Gharaibeh M., Obaidat M., Alazzam A., Meilunas M., Yin L., Anselm M., Borgsen P. (2015) LGAs VS. BGAs – Lower Profile and Better Reliability.

[21] NXP Semiconductors (2008) Introduction to the Plastic Ball Grid Array (PBGA) (read 11.10.2018), URL: https://www.nxp.com/docs/en/package-information/PBGAPRES.pdf

[22] Huber+Suhner (2008) RF Connector guide (read 15.11.2018) URL: http://pdf.directindustry.com/pdf/huber-suhner/rf-guide/30583-293499.html

[23] Rosenberger (2015) Straight plug PCB full detent [data sheet] (read 19.11.2018) URL: https://www.datasheets360.com/pdf/3688425803801746222

[24] Rosenberger (2016) Adaptor Mini SMP Jack-Jack [data sheet] (read 19.11.2018) URL: https://www.datasheets360.com/pdf/7990210905853149407

[25] Confidential Document 1, Molex

[26] Confidential Document 2, Molex

[27] Confidential e-mail conversations and meetings between Molex and Nokia

[28] Kawabata H., Hasuike K., Kobayashi Y., Ma Z. (2006) Multi-Frequency Measurements of Complex Permittivity of Dielectric Plates using Higher-Order Modes of a Balanced-Type Circular Disk Resonator. *IEEE European Microwave Conference, September 2006*

[29] Suzuki H., Inoue M. (2012) Complex Permittivity Multi-Frequency Measurements for Dielectric Sheets Using a Circular Disk Resonator. *IEEE/MMT-S International Microwave Symposium Digest, June 2012*

[30] Rosenberger (2016) SMD Connector Jack [data sheet] (read 19.11.2018) URL: https://www.mouser.fi/datasheet/2/704/08K80A-40ML5-1145218.pdf

[31] Wang X., Ding W. (2014) Back Drilling in High-Speed Interconnect System. *IEEE 15th International Conference on Electronic Packaging Technology, August 2014*

[32] Altium LLC (2018) Controlled Depth Drilling, or Back Drilling (read 16.1.2019) URL: https://www.altium.com/documentation/18.0/display/ADES/((Controlled+Depth+Drilling,+or+Back+Drilling))_AD

[33] Li W., Breier M., Aach T. (2012) Vision-Based Auto-Teaching for Automated PCB Depaneling. *IEEE 10th International Conference on Industrial Informatics, Conference 2012*

[34] Li L., Rao Y. Lin J-K. (2001) Pb-free Solder Paste Reflow Window Study for Flip Chip Wafer Bumping. *IEEE Proceedings International Symposium on Advanced Packaging Materials Processes, Properties and Interfaces, Conference 2001*

[35] Kripesh V., Kwan W. W., Iyer M. (2003) Ultra-Fine Pitch Pb-free & Eutectic Solder Bumping with Fine Particle Size Solder Paste for Nano Packaging. *IEEE Proceedings of the 5th Electronics Packaging Technology Conference (EPTC 2003)*

[36] Kangasvieri T., Komulainen M., Jantunen H., Vähäkangas J. (2008) Low-Loss and Wideband Package Transitions for Microwave and Millimeter-Wave MCMs. *IEEE Transactions on Advanced Packaging 31(1), 170-181*

[37] Polak, E. (1997) Optimization, 124, Springer

[38] Haupt, R. L. & Haupt, S. E. (2004) Practical Genetic Algorithms, Wiley

[39] Eurocircuits (2014) PCB Multi-layer Fabrication – Lay-up and Bond (read 15.3.2019) URL: https://www.eurocircuits.com/pcb-multilayer-fabrication-layup-and-bond/

[40] Mitutoyo Sheet Metal Micrometer-Series 389 – datasheet (read 2.4.2019) URL: https://ecatalog.mitutoyo.com/Sheet-Metal-Micrometers-Series-389119118-C1127.aspx

[41] Bogatin E. (2010) Signal and Power Integrity – Simplified, second edition, Prentice Hall, (pp. 193- 198)

[42] Isola Group, PCB Material Selection for RF, Microwave and Millimeter-wave Design, (pp. 12-16) URL: https://www.isola-group.com/wp-content/uploads/PCB-Material-Selection-for-High-speed-Digital-Designs-1.pdf

9 ATTACHMENTS

Attachment 1 GCPW-via-antenna S_{11}-measurement results in one figure against simulation result (highlighted with wider red line)